Master's thesis

NTNU
Norwegian University of Science and Technology
Faculty of Natural Sciences
Department of Materials Science and Engineering

Sigurd Grydeland Schawlann

High Performance Wear Resistant Bainite Steel for Agricultural Application

Master's thesis in Materials Science and Engineering
Supervisor: Ida Westermann
Co-supervisor: Erlend Sølvberg
June 2021

NTNU
Norwegian University of Science and Technology

Sigurd Grydeland Schawlann

High Performance Wear Resistant Bainite Steel for Agricultural Application

Master's thesis in Materials Science and Engineering
Supervisor: Ida Westermann
Co-supervisor: Erlend Sølvberg
June 2021

Norwegian University of Science and Technology
Faculty of Natural Sciences
Department of Materials Science and Engineering

NTNU
Norwegian University of
Science and Technology

Preface

The master thesis has been conducted at the Norwegian University of Science and Technology (NTNU) in Trondheim, at the Department of Material Science and Engineering during the spring of 2021.

Acknowledgments

I would like to extend my sincere gratitude to my supervisor Associate Professor Ida Westermann and co-supervisor Erlend Sølvberg for sharing their knowledge and expertise. Their continued guidance throughout this thesis has been essential.

I also want to thank Pål Christian Skaret and Berit Vinje Kramer for their guidance and help with sample preparation and mechanical testing.

Finally, I would like to thank my girlfriend Simone Maria Eichstetter for her endless support and encouragement throughout my five years at NTNU.

Abstract

This work is a part of the TailorPro research project, which aims to improve the understanding of heat treatment and coating technology on common and novel steel alloys. In relation to that objective, the influence of austempering time and temperature on a prototype high silicon steel, called 9022, was examined. Potential bainitic steels, such as 9022, with a large amount of silicon are often referred to as carbide-free bainitic (CFB) steel, as the silicon hinders the precipitation of carbides between the bainite laths which instead are separated by a carbon-rich retained austenite film. However, the retained austenite can also form an undesirable block structure. CFB steels have shown higher fracture toughness, strain at fracture, and improved resistance to wear, compared to martensite of similar hardness. The 9022 steel is intended for parts subjected to high abrasive wear conditions and achieving a bainitic microstructure could be an inexpensive and efficient way of improving wear resistance.

Initially, a broad experimental matrix was performed in order to get an indication of the influence of austempering time and temperature on the bainitic microstructure. Samples were austempered at temperatures between 260 and 400°C, increasing in increments of 20°C. For each austempering, four different holding times were used, 0.5, 2, 10, and 24 hours. Characterization of the development of bainite, using Vickers hardness and light optical microscopy (LOM), indicated that depending on temperature, the transformations can be separated into two categories. Samples austempered at 260 – 360°C show a reduction in hardness with increasing austempering temperature and increasing holding time from 0.5 to 2 h. Further increases in holding time have a negligible impact. However, for samples held at 380 – 400°C, these trends are inversed. 400°C was the highest austempering temperature, and it also exhibited the highest hardness. An increase in holding time, from 0.5 to 2 h, caused a significant increase in hardness.

By considering the resulting microstructure and hardness from the different austempering procedures, a subsample was chosen for further tensile- and Charpy impact testing. The selected austempering temperatures were in the range 260 – 300 and 400°C. The results indicate a stronger correlation between mechanical properties and holding time compared to holding temperature. The samples held at 260 – 300°C for 2 h had a yield strength of approximately 1100 MPa, an ultimate tensile strength (UTS) of 1650 – 1860 MPa, and a strain at fracture of 9 – 11 %. The samples held at 260°C for 2 h showed an absorbed energy of 25.4 J when Charpy impact tested, about 9 J lower than the samples held at 280 and 300°C.

The austempering holding time impacted the shape of the stress-strain curve. The yield point for the samples austempered for 2 hours was significantly lower than the samples for 0.5 and 10 h, though the UTS was similar or higher. It was suggested that this was caused by transformation induced plasticity (TRIP), in which retained austenite transforms into martensite during plastic deformation, greatly enhancing strain hardening rates. X-ray diffraction (XRD) revealed that the samples held at 280°C for 0.5, 2, and 10 h, had 14%, 18%, and 15% retained austenite, respectively. This supports the hypothesis that the TRIP-effect is occurring. By aggregating these results and considering the practical aspects, it was found that austempering at 280°C for 2 hours would achieve the most favorable combination of mechanical properties, reasonable processing time, and robustness to deviations in temperature and time.

Sammendrag

Dette arbeidet er en del av forskningsprosjektet TailorPro, som har som formål å utvide forståelsen av varmebehandlingsprosesser av nye og eksisterende stållegeringer, i den hensikt å maksimere produkters levetid. I henhold til TailorPro sin målsetting, har dette arbeidet utforsket påvirkningen austemperings-tid og -temperatur har på egenskapene til et prototype-stål med høyt silisiuminnhold. Slike bainittiske stål er ofte kalt karbidfrie bainittstål. Det høye silisiuminnholdet hindrer presipitering av karbider mellom bainittnålene og bainittnålene blir istedenfor skilt av en karbonberiket restaustenitt. Rest-austenitten kan også danne en uønsket blokkstruktur. Denne typen bainittstål har vist høyere grad av bruddseighet, tøying ved brudd og forbedret slitemotstand, sammenlignet med martensittiske stål med tilsvarende hardhet. Stålet er tiltenkt en del som er utsatt for høy grad av slitasje. En bainittisk mikrostruktur vil være en billig og effektiv måte å forbedre delens slitasjemotstand.

Det første steget av forsøket var å gjennomføre et forsøk med intensjonen om å få innsikt i hvordan austemperings -tid og -temperatur påvirker bainittens egenskaper. Prøver ble austemperert ved temperaturer mellom 260 og 400°C, med 20°C mellom hver prøve. For hver austempering ble fire ulike holdetider brukt: 0.5, 2, 10 og 24 timer. Bainittens utvikling ble undersøkt ved bruk av lysmikroskop og Vickers hardhetsmålinger. Resultatene viser to trender, avhengig av den anvendte temperaturen. For prøver som ble austemperert ved en temperatur mellom 260 og 380°C, kan man se en reduksjon i hardhet ved økt temperatur og ved å øke holdetiden fra 0.5 til 2 timer. En holdetid utover 2 timer har neglisjerbar effekt på hardhet. For prøvene som ble austemperert ved 380 og 400°C, er disse trendene invertert. 400°C var den høyeste temperaturen som ble testet og denne prøven hadde høyest grad av hardhet. En økning av holdetiden fra 0.5 til 2 timer, førte også til en betydelig økning i hardhet.

Et utvalg av de undersøkte austemperingsprosedyrene ved temperaturer mellom 260 og 300, samt 400°C, ble undersøkt nærmere ved hjelp av strekktesting og Charpyprøving. Resultatene viser en sterkere korrelasjon for de mekaniske egenskapene mellom samme holdetid, enn for lik temperatur. Prøvene som ble holdt i 2 timer ved 260 til 300°C hadde en flytespenning som var ca. 1100 MPa, en strekkfasthet som var 1650 – 1860 MPa og en 9 – 11% forlengelse ved brudd. Prøvene som ble austemperert ved 260°C i 2 timer, hadde en absorbert energi på 25.4 J i Charpyprøving. Det var ca. 9 J lavere enn prøvene som ble holdt på 280 og 300°C.

Austemperingstiden viste seg også å ha en innflytelse på formen til strekk-tøyningskurven. Prøvene som ble holdt i 2 timer hadde betydelig lavere flytespenning enn prøvene som ble holdt i 0.5 og 10 timer, men de hadde samme eller høyere grad av strekkfasthet. En hypotese var at dette skyldes transformasjons-indusert-plastisitet, en mekanisme der restaustenitt transformeres til martensitt under plastisk deformasjon, som medfører en drastisk økning i arbeidsherdingsrate. XRD viste at prøvene der denne effekten var tydeligst også hadde mest restaustenitt. Dette støtter hypotesen om TRIP-effekten. Ved å sammenfatte resultatene og vurdere de praktiske aspektene, ble det konkludert med at austempering ved 280°C i 2 timer fører til den mest fordelaktige balansen av mekaniske egenskaper, prosesseringstid og robusthet, i forhold til avvik i tid og temperatur.

Table of Contents

1 Introduction 1
2 Theory 3
2.1 The Iron-Carbon Phase Diagram 3
2.2 Phase Transformations in Steel 4
2.3 Martensite 5
2.4 Bainite 5
2.4.1 High Silicon Carbide-Free Bainite (CFB) 6
2.5 Strengthening Mechanisms in Steel 7
2.6 Alloying Elements 7
2.7 Wear 8
2.8 Process 9
3 Experimental 11
3.2 Equipment 12
3.2.1 Isothermal Holding 12
3.2.2 Tempering of Martensite 13
3.3 Sample Preparation 13
3.4 Microscopy 14
3.5 Vickers Hardness 15
3.6 Charpy Impact Test 15
3.7 Tensile Testing 16
4 Results 17
4.1 Previous Results 17
4.2 Austempering Time and Temperature 19
4.3 Microstructure 21
4.4 Tensile Testing 24
4.5 Charpy Impact Testing 27
4.6 Retained Austenite 28
4.7 Simulated Transformation Temperatures 30
5 Discussion 31
5.1 Austempering 31
5.2 Retained Austenite 32
5.3 Mechanical Properties 33
5.3.1 Tensile Testing 34
5.3.2 Charpy Impact Testing 35

5.4 Comparison with Reference Steel 36
6 Conclusion 39
7 Further Work 41
References 42
Appendices 44
7.1 A 44
7.2 B 44

1 Introduction

TailorPro is a 4-year innovation project between SINTEF and the industrial partners Kverneland Group, Nøsted & AS, and Dokka Fasteners AS. Despite producing different products, the partners share some common challenges. Their products are based on advanced steel processing, in-house forming, and heat treatment. In addition, the product lifetimes are limited by the same damage mechanisms: abrasion, stress corrosion cracking, and fatigue. Thus, TailorPro aims to improve the understanding of heat treatment and coating technology on conventional and novel steel alloys [1].

Kverneland Group is a large manufacturer of agricultural equipment, in which steel is an essential material. In the pursuit of durable products with long lifetimes, while maintaining cost control, it is essential to have a thorough understanding of physical metallurgy. Understanding the strength mechanisms of steel and the influence of different alloying elements and processing steps, makes it possible to use cheaper steels with fewer processing steps, while delivering the required quality. Because the consumption of steel is so large, it is worthwhile to invest considerable research into optimization. The benefits of minor improvements can scale up and have a significant impact on profitability.

Kverneland expressed an interest in utilizing austempered steels with a bainitic microstructure in a plough part, called a "knock-on holder". On every plough shear there is an attachable point, that cuts the soil before the mould board turns it, as seen in Figure 1-1. Because of the high levels of abrasive wear the point is exposed to, it is designed to be changed regularly. The points are attached to the knock-on holder by knocking them on using a hammer, hence the name. The knock-on holder requires resistance to abrasive wear, stress corrosion cracking, and brittle fracture. Austempering of this part could fulfill these demands at a low cost.

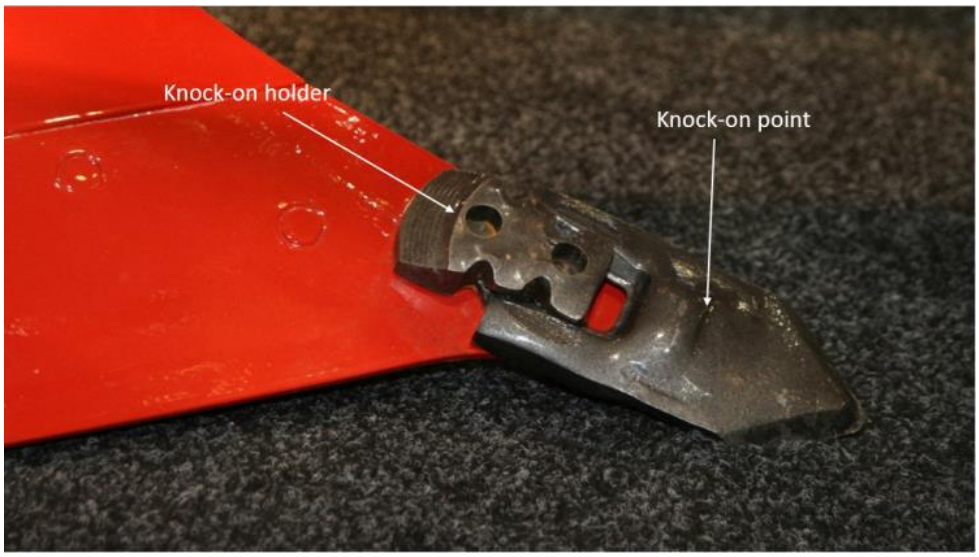

Figure 1-1 Image of a knock-on holder and -point, attached to a plough shear [2].

This work is a continuation of the project work "*Characterization of a Prototype High Performance Steel"* [3], performed by the present author at NTNU during the fall of 2020, in collaboration with Kverneland Group. The project work included identifying austenitization temperature, constructing a CCT diagram using dilatometry, and mechanical testing of the 9022-steel.

The main object of this study is to continue the characterization of this steel, with focus on bainitic microstructures, heat treatment, and comparing the bainitic properties to martensite. This characterization was done by mechanical testing of different austempering procedures, and the properties were compared with tempered martensite, with an end goal of achieving a microstructure with the potential for superior abrasive wear resistance.

Prior to austempering, the samples were austenitized at 1000°C, for 1 hour, followed by direct austempering at temperatures between 260 and 400°C. Different holding times were examined for each temperature, 0.5, 2, 10, and 24 hours. After austempering, the Vickers hardness was measured, and the microstructure was examined. The hardness measurements were used to select samples for further examination and mechanical testing. Tensile testing and Charpy impact testing were conducted on samples held at different times at 260, 280, 300, and 400°C. The high silicon content in the steel in question leads to greater amounts of retained austenite in bainite, which has a significant influence on the mechanical properties. In order to identify the amount and distribution of retained austenite, electron backscatter diffraction (EBSD) and XRD was used.

Finally, the bainitic steel was compared with the steel that is currently used in the production of knock-on holders, quenched 30M12CB. Because austempering of 9022 would require an extra processing step, compared to the direct quench of 30M12CB, the quality gain should be substantial.

2 Theory

This section is dedicated to presenting relevant theory for this thesis. The aim is to introduce phase transformations and strengthening mechanisms in steel, with a particular focus on how these are influential in bainite.

2.1 The Iron-Carbon Phase Diagram

Any exploration of the properties of steel starts by understanding the iron-carbon phase diagram, as presented in Figure 2-1. This diagram is not an equilibrium phase diagram; it is more adapted to practical application. The true equilibrium phase of carbon is graphite, not cementite, but the transformation time is so long it does not have practical relevance. The properties of the phases and transformation points can change by the addition of alloying elements.

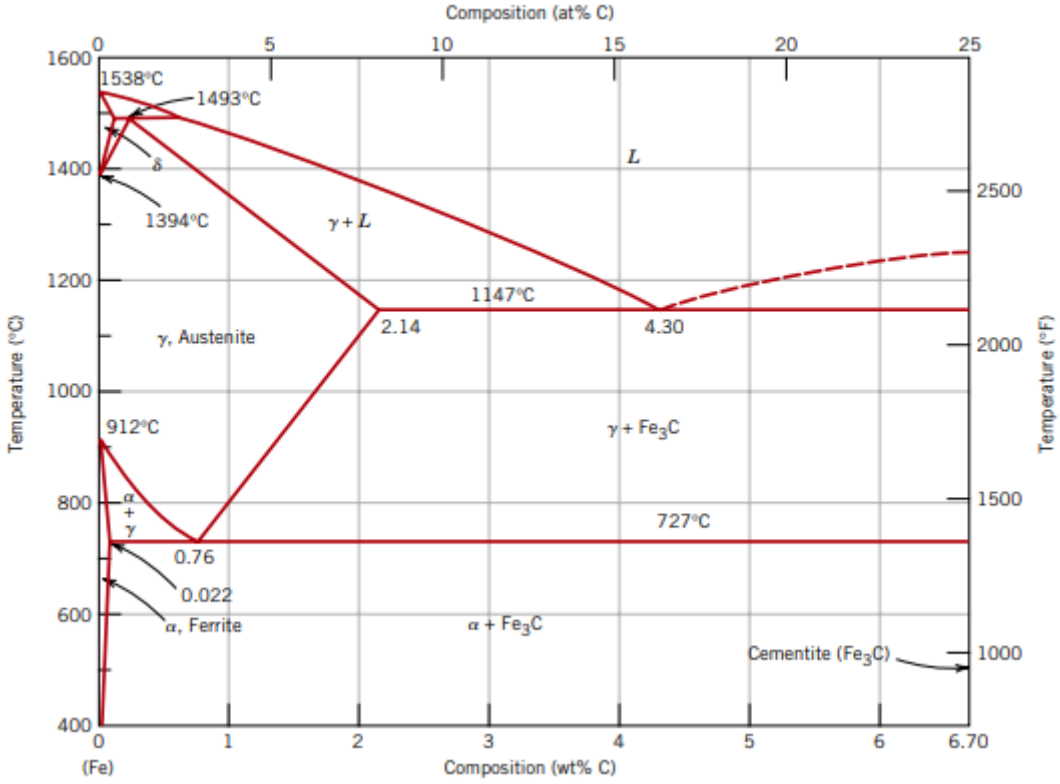

Figure 2-1 The iron-carbon phase diagram [4].

In this thesis, and most other works, ferrite (α), pearlite and austenite (ɣ) are the most important phases. At room temperature, the equilibrium phase of iron is ferrite. Ferrite has a body-centered cubic (BCC) structure. BCC structures have a low solubility for interstitial atoms. If the carbon content exceeds the maximum solubility of 0.02 wt%, the carbon precipitate out and form cementite (Fe_3C). The cementite forms a lamellar structure with ferrite that is called pearlite. At temperatures above A_1, austenite starts to form. The ferrite to austenite phase transformation is characterized by a transformation of the crystal structure from body-centered cubic (BCC) to face-centered cubic (FCC).

2.2 Phase Transformations in Steel

Although phase diagrams are useful tools, they have one crucial weakness; they do not account for the kinetics of a phase transformation. As a steel is cooled below A_1, it does not instantly form ferrite or pearlite. Different phases are produced depending on temperature and time. In order to identify the expected phase, time-temperature-transformation (TTT) diagrams are used, as shown in Figure 2-2. Which transformations that occur are determined by two factors: the temperature and the driving force of the reaction. These two factors are inversely related to each other. If the austenite is at temperatures far below A_1, called high under-cooling, the driving force of the transformation is high. However, the available energy for diffusion is low due to the low temperature. At temperatures just below A_1, called low under-cooling, the case is the opposite; the available energy for transformation is high, but the driving force of the reaction is low. This gives the TTT-diagram the "C" shapes. At the tip of each "C", these factors combine; the transformation rate is highest, and any deviation in temperature results in lower transformation rates.

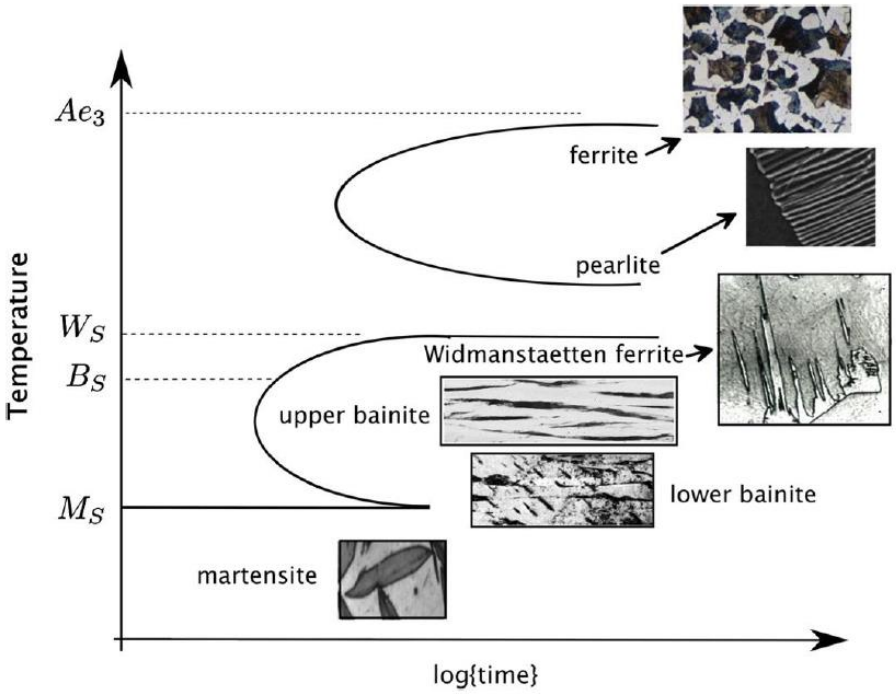

Figure 2-2 A TTT-diagram for steel that illustrating microstructures that can be achieved in principal [5].

At high temperatures and a long holding time, an equilibrium ferrite/pearlite microstructure will form. This transformation is only driven by diffusion. The transformation to ferrite starts at grain boundaries or inclusions; the excess carbon diffuses into the austenite grains until it reaches eutectic composition. At this point, carbon diffuses interstitially from the austenite to the tip of the cementite, forming a lamellar cementite/ferrite structure. This structure is called pearlite.

2.3 Martensite

Martensite is formed at high cooling rates, and it transforms without any diffusion. By cooling the austenitic steel fast enough, there is no time for diffusion to occur. The carbon is "trapped" within the austenite matrix, but the austenite is still unstable. In this case, the austenite transforms by a shear deformation. The FCC structure of the austenite transforms into an elongated cubic structure, called body-centered tetragonal (BCT). This transformation causes a volume increase of up to 4%. Martensite can also form due to plastic deformation of the austenitic phase. Steel that contains high amounts of retained austenite, that deform during deformation, are called transformation induced plasticity (TRIP) steels [5].

Martensite is the hardest, most brittle phase in steel, caused by the combination of the supersaturated interstitial carbon, with the large number of dislocations induced during shear deformation. In this state the steel is too brittle for most applications. By tempering the martensite, the toughness is improved, with a slight reduction in hardness. The tempering occurs in five steps [6]:

1. 100-150^{o}C: if the carbon content is larger than 0.2wt%, ε-carbides precipitate out of the martensite.
2. 250-325^{o}C: retained austenite transforms into martensite or austenite.
3. 325-400^{o}C: cementite forms and ε-carbides transform into cementite.
4. Recovery and recrystallization of the martensitic microstructure. Vacancies and dislocations are eliminated.
5. Above 450^{o}C: alloy carbides form in high alloy steels.

It is important to note that these temperatures are for plain carbon steel, the addition of alloying elements can influence the temperatures at which the different steps occur.

2.4 Bainite

Bainite is formed at intermediate temperatures during cooling from austenite, between the transformation of pearlite and martensite, typically in the range of 250 and 550^{o}C [5]. Bainite consists of aggregated ferritic plates that are separated by martensite, retained austenite, or cementite. These aggregates are called sheaves. There is still uncertainty of whether the formation of bainite is displacive or diffusion-controlled [5]. It

has been shown that bainite can transform at temperatures as low as 125°C over tens of days. The maximum diffusion distance for this process is 10^{-17}m [7].

Describing the different morphologies is also not straightforward, as bainite can have morphologies that are similar to martensite or ferrite. However, two main categories of bainite have been established: upper and lower bainite. These categories are determined by the precipitation of carbides, illustrated in Figure 2-3. Upper bainite is formed at higher temperatures, causing carbon to diffuse, and carbides are formed between the bainitic plates. Lower bainite is formed at lower temperatures, which causes slower diffusion and the carbides precipitate within the plates.

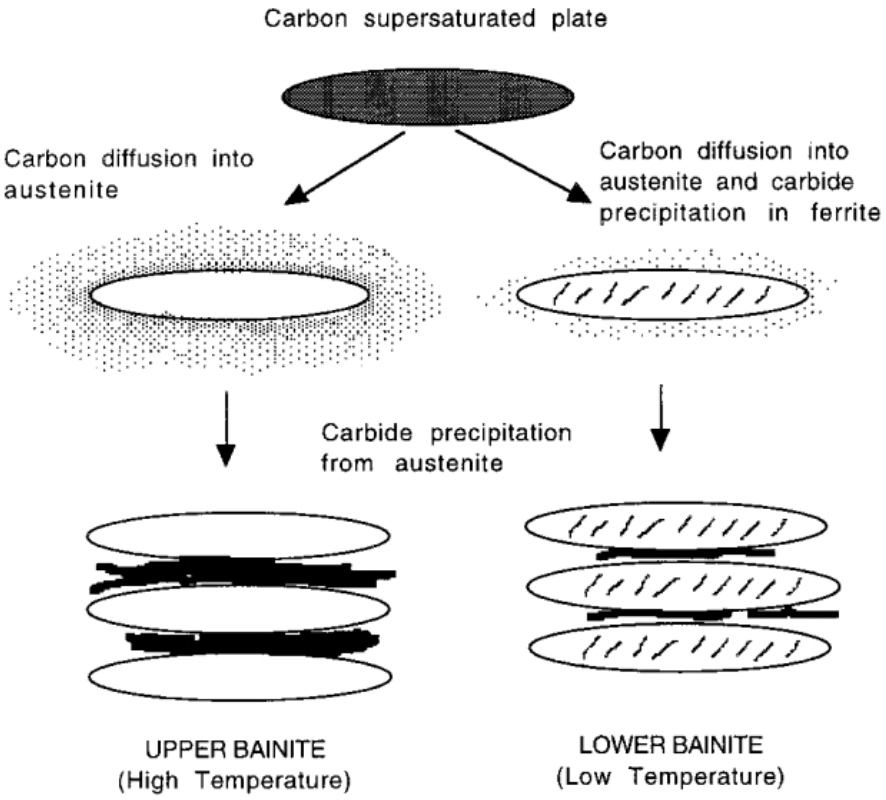

Figure 2-3 Illustration of the transition to upper and lower bainite [5].

2.4.1 High Silicon Carbide-Free Bainite (CFB)

Bainitic steels with high silicon content are classified as carbide-free bainite (CFB). Instead of carbides precipitating at the grain boundaries, retained austenite separates the bainitic laths. Retained austenite in CFB steel is caused by Si inhibiting precipitation of carbides [8]. At the austempering temperatures, austenite has a much greater solubility of carbon compared to ferrite [9]. This causes carbon to diffuse from the growing bainite into the surrounding retained austenite. The higher carbon concentration stabilizes the austenite and the bainite transformation stops, which prevents the final step of the reaction in Figure 2-3 from occurring. This process is called the incomplete reaction phenomena, and it provides a limit to the amount of bainite that can form [10].

Retained austenite usually takes two shapes, either as a thin film between the bainite laths or blocky areas, typically at the previous austenite grain boundaries. The thin film structure is favorable because it is more mechanically stable compared to blocky austenite [11]. These films are stable and can greatly improve mechanical properties [12]. Austenite has high formability that can inhibit the propagation of cracks by absorbing more energy, and a different crystal structure, retained austenite (FCC) compared to bainite (BCC), which hinders dislocation movement [13]. The retained austenite also impedes the diffusion of hydrogen in the steel [14]. The result of this can be a steel with high hardness, toughness, and elongation.

2.5 Strengthening Mechanisms in Steel

There are several mechanisms that ensure the properties of steel, such as work hardening, grain refinement, precipitation-, and solid solution strengthening.

Work hardening is caused by the formation of dislocations by plastic deformation. A dislocation causes a local change in the stress field around it, that inhibits the movement of other dislocations. The limit of work hardening occurs when the rate of dislocation annihilation is equal to the rate of dislocation creation. It is possible to increase the tensile strength of a low carbon steel by up to 550 MPa, by a 95% reduction in cross-section.

Precipitation strengthening is caused by the presence of small phases in the matrix. They are typically carbides, nitrides, or intermetallic compounds. The precipitates can have different effects on the properties of the steel, depending on size, shape, and distribution. Small semi-coherent precipitates, that are finely distributed throughout the matrix, can strengthen the steel by hindering dislocation movements. Some precipitates can be coarser and precipitate out at higher temperatures. The presence of these particles can retard grain growth during heat treatment [5].

The grain structure of a steel can have a profound impact on strength and phase transformations. Reducing the grain size of a steel is usually done by adding micro alloying elements, that produce the retardation of grain growth mentioned above, in combination with thermomechanical rolling [15]. This is a widely used process because it is inexpensive, reliable, and scalable.

2.6 Alloying Elements

Carbon is the most important alloying element in steel. The addition of carbon increases hardness and tensile strength, but it reduces ductility and toughness. Carbon has a significant impact on the formation and properties of bainite and retained austenite. During the formation of bainite, carbon diffuse out of the bainite, either due to precipitation or partitioning into the surrounding austenite. Both mechanisms can occur simultaneously; t. The dominating process depends on the temperature and alloying elements.

Long, Kang [16] examined the properties of carbide-free medium carbon steels. The steels they examined had bulk carbon concentrations before austempering of 0.34 wt%,

while after different austempering processes, the carbon concentration in the retained austenite was 1-1.2 wt%. The partitioning of excess carbon into the austenite is not homogeneous. The carbon concentration in retained austenite is higher in the vicinity of bainite platelets. This variation in concentration causes local differences in the stability of the retained austenite; the areas with higher carbon concentration have lower martensite start temperature (M_s) and higher mechanical stability [9]. The varying carbon distribution is an important factor for the difference in stability of retained austenite as blocks or thin films. The thin films are closer to the bainite laths and therefore higher in carbon, and more stable.

Silicon is a common alloying element in newer advanced high strength steels (AHSS)., In for examplesuch as carbide-free bainitic steel, silicon is a common alloying element. Silicon is a ferrite stabilizer and, requiresing a higher temperature for a full austenitizing. While silicon stabilizes ferrite during heating, it increases hardenability during cooling and can cause higher fractions of retained austenite in carbide-free bainitic steels. The reason for this is that silicon is a strong precipitation inhibitor. In addition to that, silicon also reduces surface quality as it increases decarburization during austenitization.

Chromium and manganese are the cheapest way of increasing the hardenability of a steel [5] by inhibiting the formation of pearlite. However, it has been shown that manganese can reduce the rate of the bainitic transformation. Huang, Sherif [17] found that a low-Mn and high-Cr steel had a significantly accelerated bainite transformation.

Manganese is added to steel to avoid hot shortness. Hot shortness is caused by the presence of sulfur, which forms iron sulfide on the grain boundaries. Iron sulfide has a melting point of 988^{o}C. If the steel is deformed at this temperature, the molten iron sulfide film reduces formability, and the steel becomes brittle. By adding manganese, the sulfur primarily binds to the manganese, forming particles with a higher melting point [15]. Manganese can also be added, in amounts up to 25 wt%, to stabilize austenite in 2. generation TRIP steel [18].

2.7 Wear

Wear is the process of progressive loss and deformation of a material, caused by relative movement between surfaces [19]. Identifying the wear resistance of a steel is a complex process that requires testing that is tailored to the specific environment in which the wear occurs. One of the reasons for the difficulty of simulating wear is that wear is a "system property" where mechanisms such as abrasive wear, corrosion, impact abrasion, surface fatigue, and adhesion, can occur simultaneously and influence each other, leading to unpredictable results [19]. Nevertheless, by examining the relevant theory, the goal is to get an understanding of which steels that can warrant further testing. In Figure 2-4, the reduction of the dimensions of a tine point is visible. The knock-on holder is designed to hold and allow for easy swapping of tine points.

Figure 2-4 Differences in dimensions between a worn and new tine point [19].

The composition of the soil where the plough is used can vary greatly and can have a significant impact on wear. Abrasion is the dominating wear mechanism, and increased hardness is correlated with higher abrasion wear resistance [20]. The pursuit of lower wear by increasing hardness has to be balanced with achieving sufficient fracture toughness in case the plough hits a larger rock. It has been shown that bainitic steels with a high amount of retained austenite can have excellent wear properties. Kumar, Dwivedi [21], found that higher amounts of retained austenite in carbide-free bainitic steels led to improved sliding-wear resistance. Liu, Li [13], studied impact-abrasion wear on similar steels. They found that improved mechanical stability of retained austenite contributed to higher wear resistance, up to the point where the retained austenite was too stable to fully transform to martensite during deformation. They hypothesized that this improvement was caused by two mechanisms; the austenite transforming into untempered martensite with high hardness and the volume increase associated with the martensite transformation. This volume expansion causes a compressive residual stress on the surface that suppress crack initiation and propagation.

2.8 Process

Most steels are produced by continuous casting and hot rolling. This is an inexpensive and effective process that is suitable for large-scale manufacturing. As the molten steel solidifies, the distribution of alloying elements might not be homogeneous. Some areas can have a significant change in chemical composition. As the steel is hot rolled, these areas are stretched out, resulting in a band-like structure with different chemical compositions. These bands are called segregation bands [22]. The propensity to form segregation bands can vary for different alloying elements, but it has been found that Mo, Cr, Mn, and Si can exhibit such behavior. The change in chemical composition can cause local differences in the mechanical and/or transformation properties.

3 Experimental

In this thesis, a high silicon steel from Ovako, with designation 9002, has been examined. The material was delivered as a rod with a diameter of 22 mm, with an unknown heat treatment. The chemical composition has been provided by the manufacturer and is presented in Table 3-1.

Table 3-1 The chemical composition of the 9022 - steel, as specified by the manufacturer. Values are shown in wt%.

	C	**Si**	**Mn**	**P**	**S**	**Cr**	**Ni**	**Mo**	**V**	**Ti**	**Cu**	**Al**
wt%	0.49	3.30	0.87	0.007	0.001	1.19	0.59	0.14	0.152	0.010	0.12	0.013

The 9022 - steel has been compared to the steel that is currently used in production at Kverneland. The steel is also supplied from Ovako, with designation 30M12CB. From here on out, this steel will be referred to as "reference". The reference samples have been subjected to the same heat treatment for all the experiments, austenitizing at 900°C for 1 hour followed by quenching in water. The material was delivered as a rod with a diameter of 40 mm. The chemical composition has been provided by the manufacturer and is presented in Table 3-2.

Table 3-2 The chemical composition of the reference steel, 30M12CB, as specified by the manufacturer. Values are shown in wt%.

	C	**Si**	**Mn**	**P**	**S**	**Cr**	**Ti**	**Al**	**B**
wt%	0.28	0.22	1.32	0.016	0.007	0.42	0.043	0.005	0.0026

3.1 Equipment

The main instruments utilized in this work are presented in Table 3-3.

Table 3-3 The instruments utilized and their purpose.

Instruments	**Purpose**
Nabertherm HTCT 08/16	Used for austenitizing samples
Innovatest manual hardness testing machine	Vickers hardness measurements
Leica VHMOT	Micro Vickers hardness measurements
Zeiss Axio 2	Light optical microscope
Zeiss - Ultra 55 - FEG-SEM	Scanning electron microscopy
Salt bath	Tempering and austempering
MTS 810Hydraulic tensile testing machine 100kN	Tensile testing

3.1.1 Isothermal Holding

In the previous work, it was found that the required temperature for a fully austenitic microstructure is 1000°C [3]. The samples were held at this temperature for 1 hour. The samples were entangled in steel wire in order to easily transfer the samples from the austenitizing oven to the salt baths. All the samples were transferred to the salt baths before they cooled down and while still glowing red.

In order to get an impression of how austempering time and temperature influence the mechanical properties of the bainite, the following experiment was conducted. Samples with a thickness of roughly 1 cm were cut from the rod. To ensure the samples had the same microstructure, they were heated to 1000°C for 1 hour and then quenched in water. Then the samples were heated again to 1000°C and held for 1 hour. After austenitizing, the samples were put in salt baths and held for different amounts of time. The samples were held at temperatures between 260 and 400°C, increasing in 20°C increments. For each temperature, 4 samples were held for different amounts of time, 0.5, 2, 10, and 24 hours, resulting in 32 different samples. This process is illustrated in Figure 3-1. After the samples were removed from the salt bath, they were cooled in air.

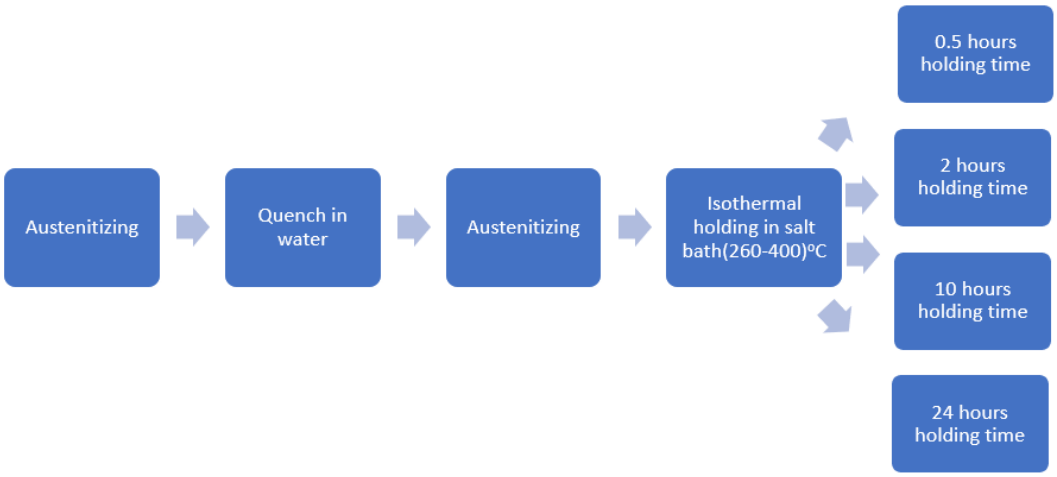

Figure 3-1 Illustration of the process in the isothermal transformation experiment.

3.1.2 Tempering of Martensite

Tempering of martensite was conducted in the same way as isothermal holding, except that the samples were quenched in water between the heat treatments.

3.2 Sample Preparation

After heat treatment, the samples were cut in half, resulting in a surface along the rolling direction without decarburization, as presented in Figure 3-2 and Figure 3-3. The samples were cold-molded in epoxy, ground, and polished with the steps shown in Table 3-4.

Table 3-4 The polishing steps prior to etching, OP-U polishing, or electro polishing.

Surface	**Lubrication**	**Time [min]**
Piano 220	Water	2
Allegro	DiaPro Allegro/largo, 9 µm	3
Dac	DiaPro Dac, 3 µm	3
Nap	DiaPro Nap-B1, 1 µm	1

After polishing, the samples were etched with 2% nital. The etching time was not determined by a set time, instead the nital was removed when the color of the surface changed, typically after 10-40 seconds. An example of a finished sample is shown in Figure 3-4. The stripes on the surface are due to segregation bands formed during production.

Figure 3-2 Image of a sample prior to heat treatment

Figure 3-3 Image of a sample after heat treatment and cutting.

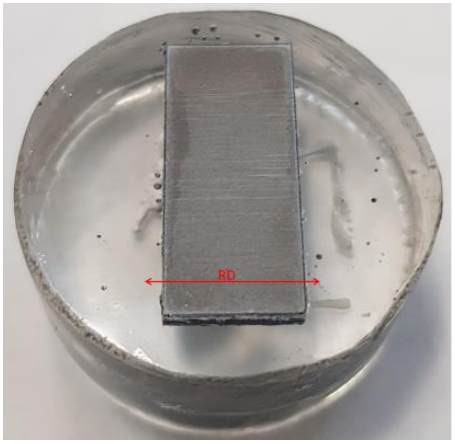

Figure 3-4 Image of a sample molded in epoxy after polishing and etching. RD indicate rolling direction.

The samples used for EBSD and XRD had a slightly different process. They were both polished down to 1 µm. Afterward, the samples for EBSD were polished with Struers OP-U for 1 minute. The samples that were examined using XRD were first mechanically polished to 1 µm and then electropolished. The following settings were used for electropolishing: A3 electrolyte, 63 V, flow rate 13, and a time of 18 s.

3.3 Microscopy

Several different imaging techniques have been utilized in this work, such as LOM, SEM (secondary electrons, backscatter electrons, and EBSD), and XRD. XRD and data analysis were conducted with the help of Maria Tsoutsouva.

Brightfield LOM was used to observe the microstructure and segregation bands, as well as qualitative observations on retained austenite. Because LOM is easy and fast, it was used to get a broad overview of the effect of heat treatment on the microstructure. Then the images from LOM could be used to identify samples of particular interest that are examined further.

Aa Zeiss Ultra 55 Field Emission SEM was used to capture higher resolution images of the microstructure to identify different phases. It was used on the samples held at 400°C to identify martensite and bainite, and on the sample held at 280°C – 2h in order to identify the distribution of retained austenite.

EBSD acquisition was performed with a Zeiss Ultra 55 Field Emission SEM, using a NORDIF UF-1100 detector. The samples were tilted at a 70° angle. The examined sample was austempered at 280°C for 2 hours. The settings for EBSD are shown in Table 3-5. Due to technical issues with the SEMs, only two EBSD-acquisitions were conducted.

Table 3-5 Settings for EBSD-acquisition of the 280°C – 0.5 h.

Magnification	500 X	2500 X
Accelerating voltage	17 kV	17 kV
Working distance	24.7 mm	24.8 mm
Area	500 µm x 500 µm	100 µm x 100 µm
Step size	1.5 µm	0.3 µm

3.4 Vickers Hardness

Hardness is used to refer to a material's resistance to localized plastic deformation. Vickers hardness measurements are done by pressing a pyramid-shaped diamond into the metal with a known force and measuring the diagonals of the indentation. In this work, hardness measurements have been conducted with a load of 10 kg, and microhardness has been measured with a load of 100 g.

3.5 Charpy Impact Test

Charpy impact test measures the absorbed energy during fracture. It is conducted by hitting a specimen with the geometry shown in Figure 3-3. The geometry of the notch can vary for different tests. The V-notch is used in this experiment, according to ISO 148-2:2016 [23].

The samples for tensile testing were only austenitized once in order to reduce decarburization and the possibility of warping during cooling. 3 parallels were tested for the austempering and the tempered martensite, for the air-cooled samples only 2 parallels were tested.

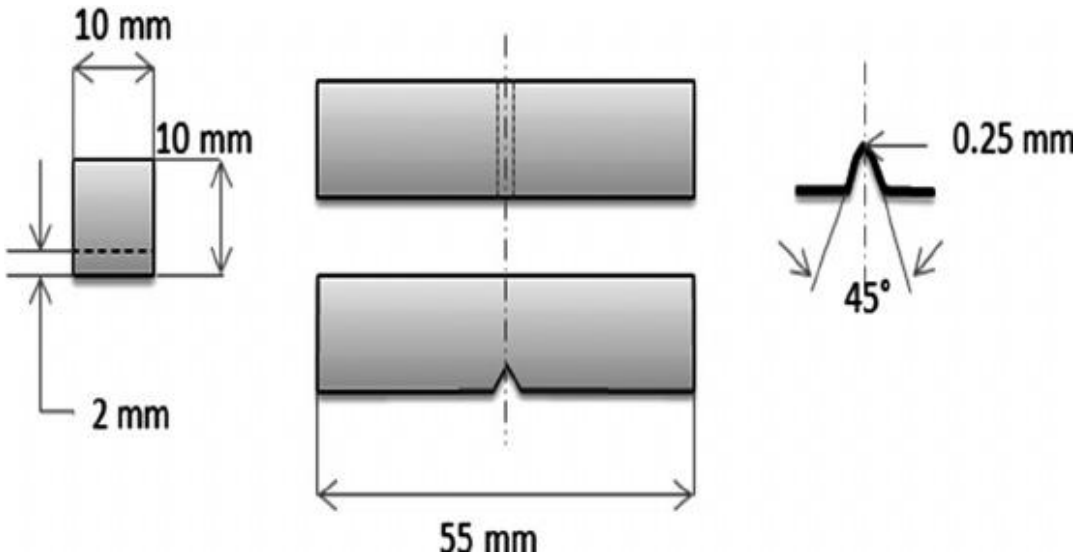

Figure 3-5 The geometry of the Charpy impact test samples.

3.6 Tensile Testing

Tensile testing identifies the properties of a material during tension. Tensile testing measures the properties yield strength, ultimate tensile strength (UTS), and maximum elongation, by applying a tensile force and measuring the elongation with an extensometer. The samples for tensile testing were only austenitized once in order to reduce decarburization and the possibility of warping during cooling.

In this experiment the gauge length of the extensometer was 25 mm, and the strain rate was 1 mm/s. The geometry of the samples that were used is shown in Figure 3-6. 3 parallels were tested for each selected heat treatment.

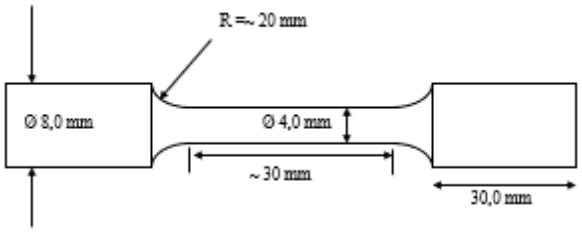

Figure 3-6 Illustration of the dimensions of the tensile test sample.

4 Results

This section is dedicated to presenting the experimental results, including Vickers hardness, Charpy test, tensile strength, and imaging using LOM and SEM. A summary of the results from previous work on the 9022-steel will also be presented.

4.1 Previous Results

In the following section, relevant results from previous work are showcased [3]. The results have influenced the decisions and procedures in this thesis. The work focused on characterizing the 9022 steel in preparation for this work, including characterizing segregation bands, finding the austenitizing temperature, constructing a CCT-diagram, and mechanical testing with martensitic microstructure.

A challenge with characterizing this steel is the prominent presence of segregation bands. This changes the properties locally, resulting in different mechanical properties and transformation temperatures.

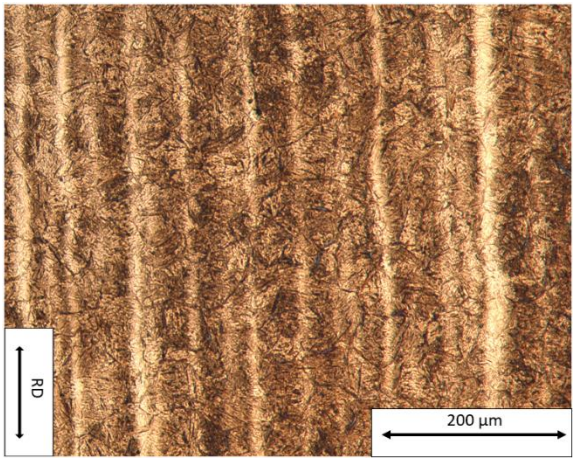

Figure 4-1 Martensitic microstructure, visible segregation bands

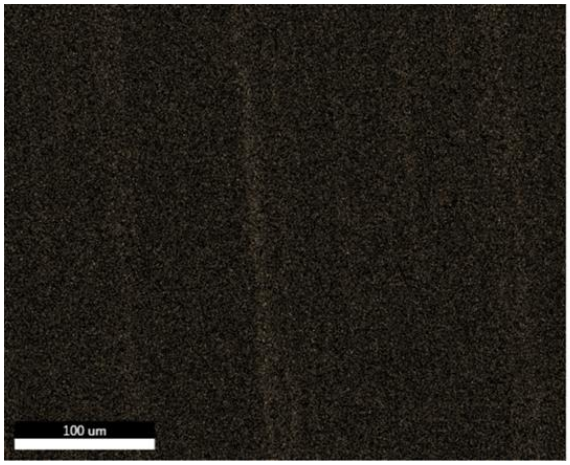

Figure 4-2 EDS-mapping of the steel as delivered. Light areas indicate silicon

Due to increased Si-content in the segregation bands, a high temperature is required to achieve a fully austenitic microstructure. By measuring hardness and using LOM, it was found that 1 hour at 1000°C would lead to a microstructure with no ferrite.

Attempts were made to identify the previous austenite grain size (PAGS). An image of the PAGS is shown in Figure 4-3. It is difficult to get accurate and representative measurements of the PAGS, because of the influence of the segregation bands. The difference in etching is stronger between the segregation bands than the PAGS, and the grain boundaries are also often overlapping with the segregation bands.

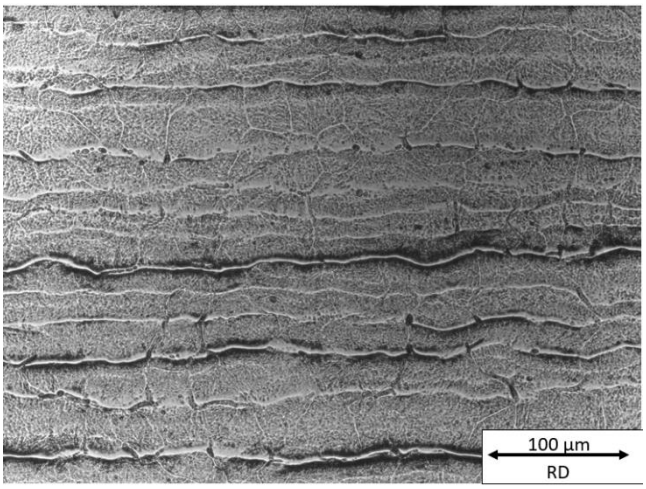

Figure 4-3 9022 austenitized at 950°C and quenched. Etched with picric acid. Previous austenite grain size.

A CCT-diagram was constructed using a Gleeble 38000-GTC system with dilatometric measurements. The dilation was measured for cooling rates between 100 and 0.5°C/s. The steel exhibited high hardenability, resulting in a martensitic microstructure for all cooling rates, except 0.5°C/s.

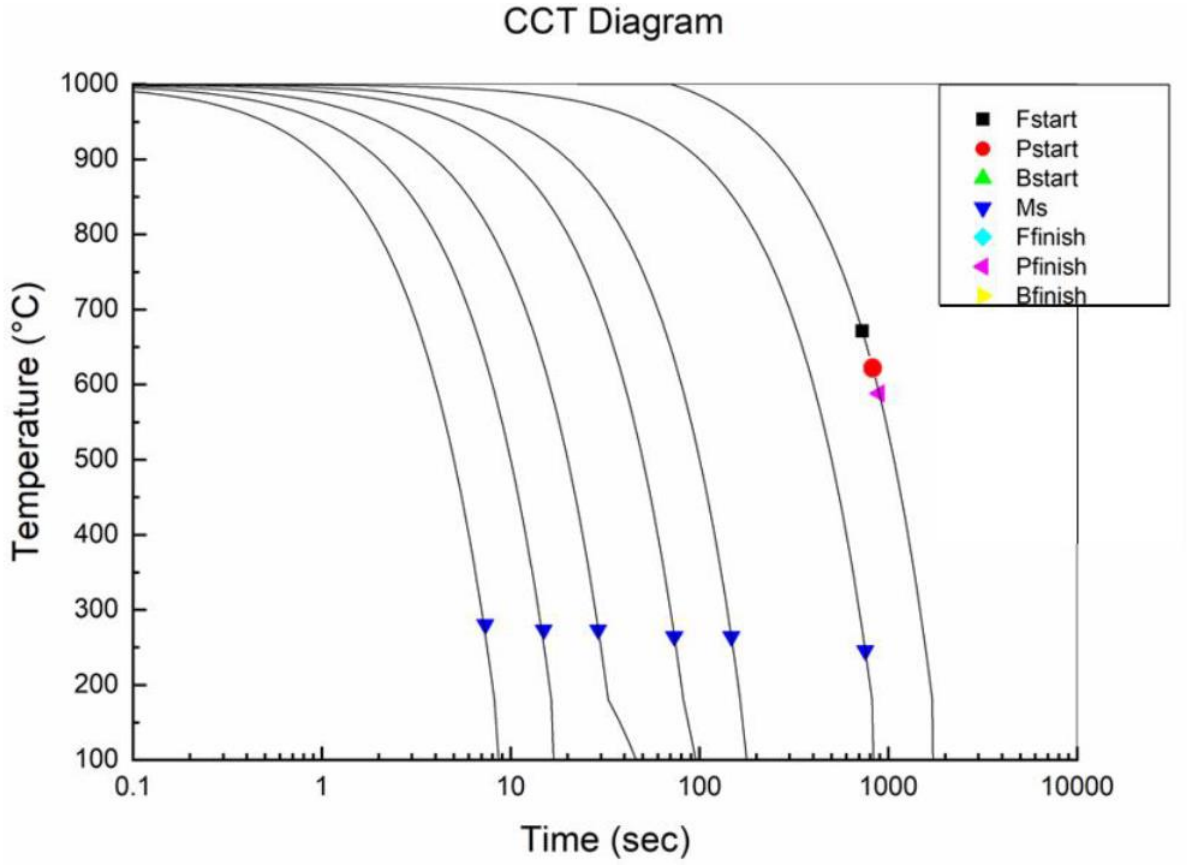

Figure 4-4 CCT-diagram for the 9022 steel. Constructed using dilatometric measurements.

Tensile, Vickers hardness, and Charpy testing were conducted on three martensitic samples: with no tempering, 1 hour at 200°C, and 1 hour at 250°C. For ease of comparison, the results will be presented with the mechanical testing conducted in this thesis.

4.2 Austempering Time and Temperature

The measured hardness of the samples, based on isothermal holding time and temperature, is presented in Figure 4-5. For the holding temperatures between 260 and 360°C, there are two apparent trends in the hardness:

- As the isothermal holding temperature increases, the hardness decreases.
- Holding times between 2 and 24 hours do not influence the hardness to a relevant degree. However, a holding time of 0.5 hours results in comparatively higher hardness.

At the highest tested temperatures, 380 and 400°C, these trends invert. Increasing temperatures and changing the holding time from 0.5 hours to 2 hours result in higher hardness.

The measured hardness of the martensitic samples is shown in Table 4-1. Tempering at 400°C results in higher hardness than 350°C, but it is within the standard deviation.

Table 4-1 Vickers hardness for steels with martensitic microstructures.

Tempering temperature [°C]. Held for 1 hour	**HV10**	**Standard deviation**
200°C*	718	6.1
250°C*	692	27.7
350°C	601	11.4
400°C	609	11.5
450°C	572	15.1
500°C	535	6.5
No tempering*	782	3.7
Reference	540	14.4

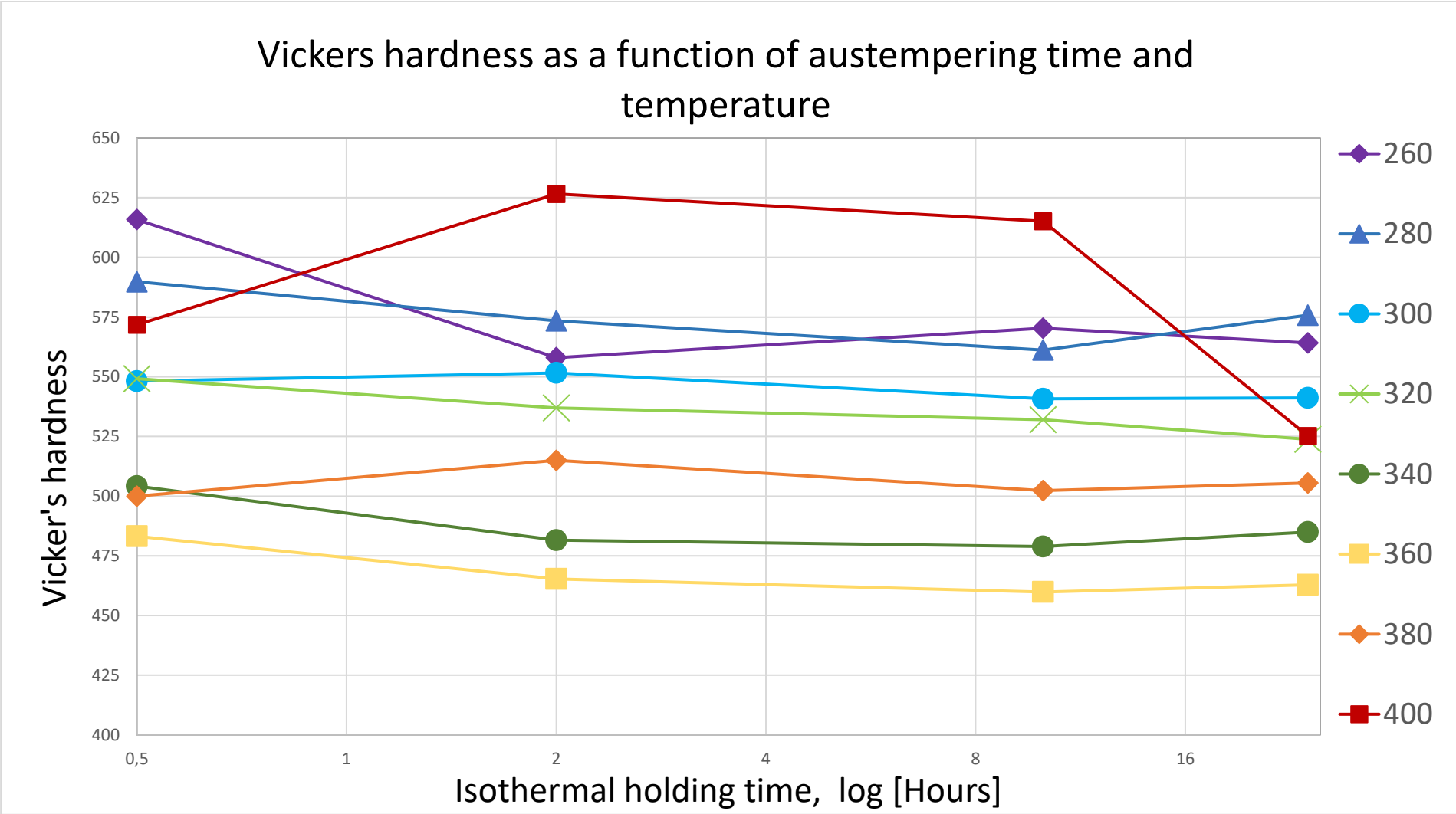

Figure 4-5 HV10 as a function of austempering time and temperature.

4.3 Microstructure

After hardness was measured, the microstructure was examined using LOM. A selection of the images is presented in this chapter, with the goal of giving some insight in to the trends observed with the hardness measurements. Figure 4-6 to Figure 4-9, shows the evolution of the microstructure as the holding time increases for samples held at 280°C. The variation in color within each image is due to a difference in etching, caused by different chemical composition in the segregation bands. In Figure 4-6, there are white spots within the needle structure, the concentration of these spots subsides with longer holding time. After 10 hours there are no traces of the white spots.

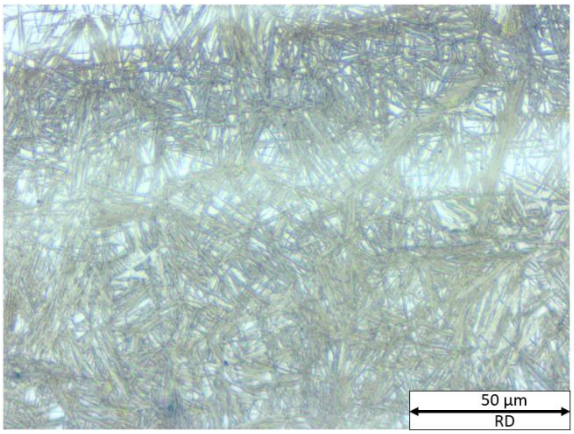

Figure 4-6 LOM. 280°C – 0.5h. Nital etch. 500X.

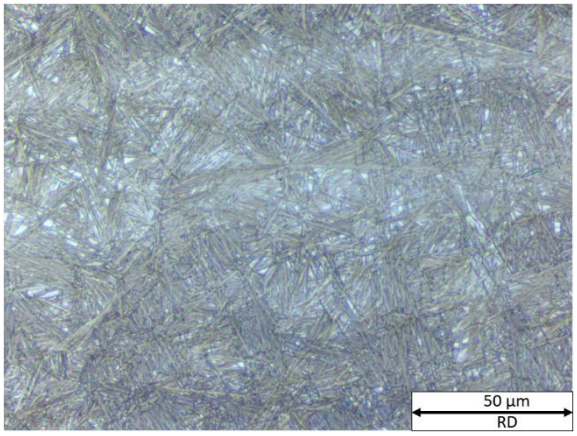

Figure 4-7 LOM. 280°C – 2 h. Nital etch. 500X.

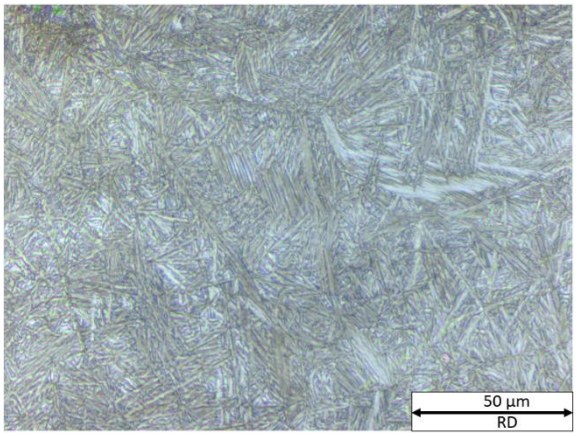

Figure 4-8 LOM. 280°C – 10 h. Nital etch. 500X.

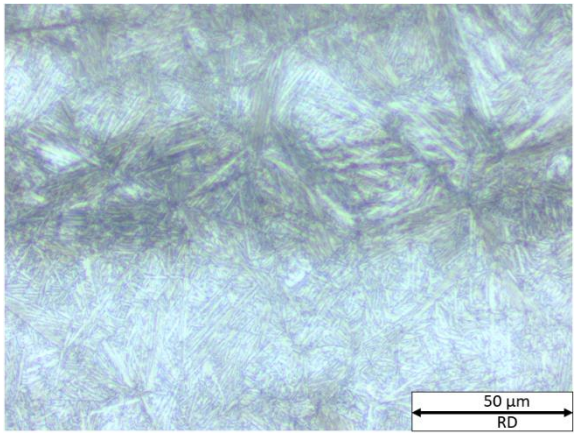

Figure 4-9 LOM. 280°C – 24 h. Nital etch. 500X.

In Figure 4-10 to Figure 4-13, the holding time is increased to 300°C. The white spots are still present, though with a lower concentration and they subside faster than at 280°C.

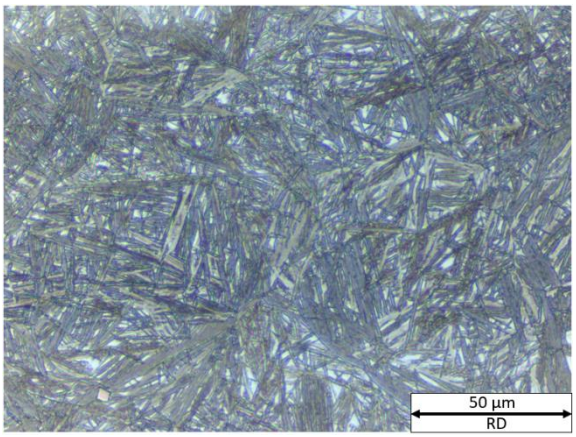

Figure 4-10 LOM. 300°C 0.5 h. Nital etch. 500X.

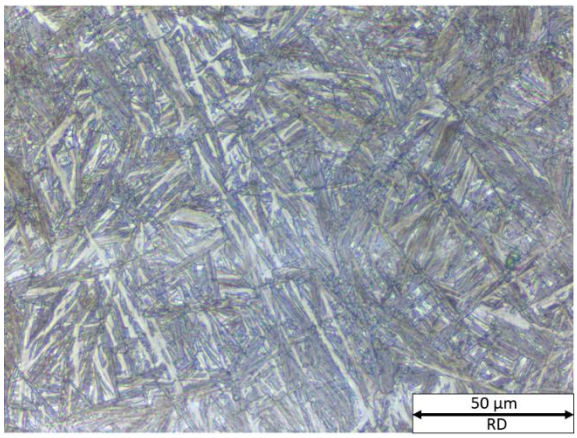

Figure 4-11 LOM. 300°C 2 h. Nital etch. 500X.

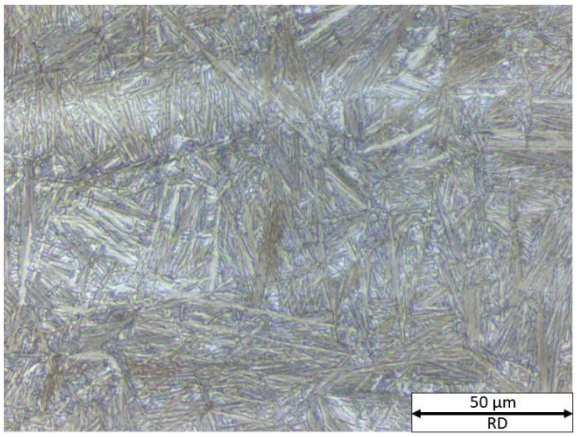

Figure 4-12 LOM. 300°C 10h. Nital etch. 500X.

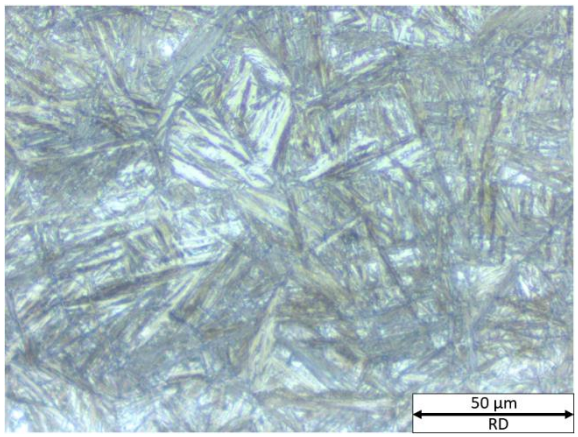

Figure 4-13 LOM. 300°C 24h. Nital etch. 500X.

The microstructure of 400°C – 2h is characterized by thick dark needles and white/brown areas, as visible in Figure 4-14 to Figure 4-17. In Figure 4-17 thin needles can be seen in between the bainite laths. Microhardness measurements of 400°C – 0.5h, gave a hardness of 558 HV0.1 for the dark needles, and 712 HV0.1 for the white/brown areas. The dark needles are most likely upper bainite, while the white/brown areas are presumably martensite. The indentations from hardness measurements of 400°C - 2h and 24h, were examined using LOM to explain the reduction in hardness. The images show that the white/brown needle structure has disappeared in the 24h sample and is replaced by what is most likely retained austenite.

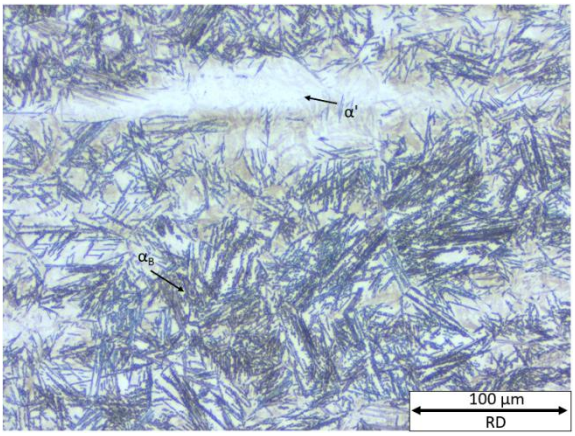

Figure 4-14 LOM. 400°C – 2h. Nital etch. 200X

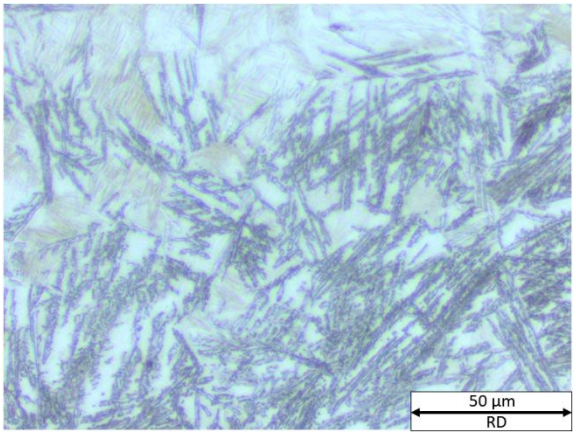

Figure 4-15 LOM. 400°C – 2h. Nital etch. 500X

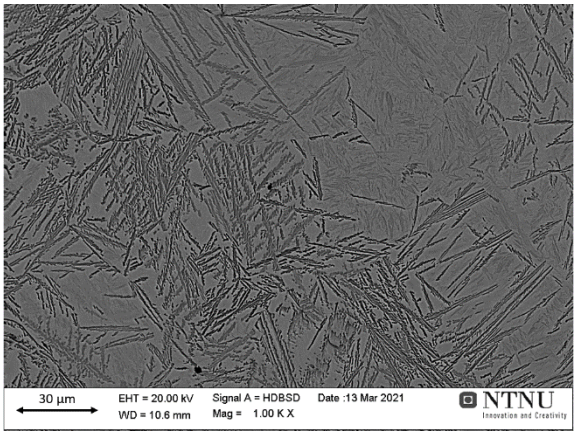

Figure 4-16 BSE. 400°C – 2h. Nital etch. 1000X

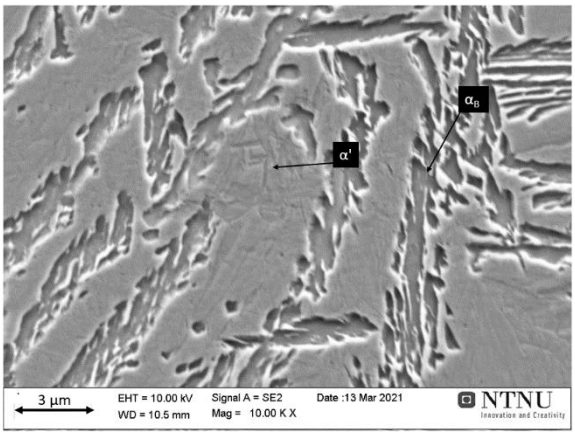

Figure 4-17 SE. 400°C – 2h. Nital etch. 10 000X

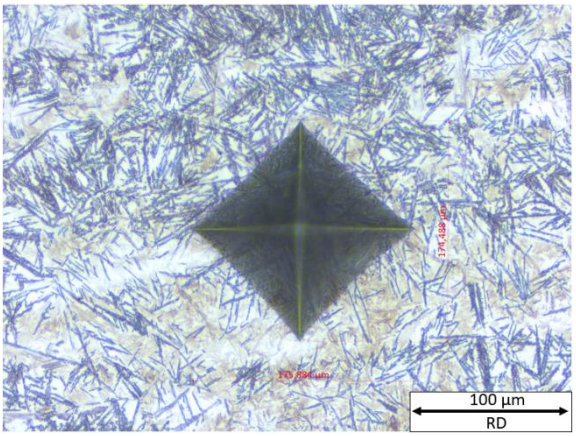

Figure 4-18 LOM. 400°C - 2h. Vickers indent 652 HV10. Nital etch. 200X

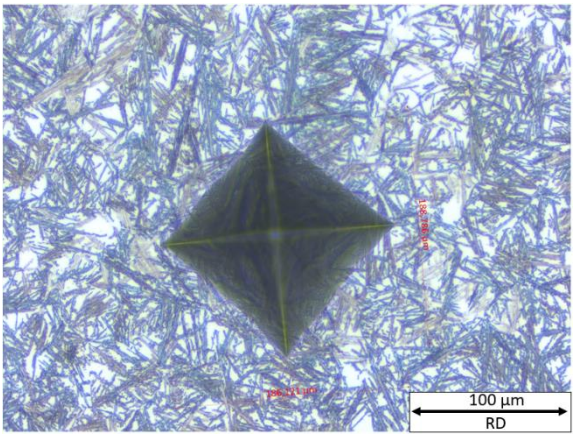

Figure 4-19 Lom. 400°C – 24h. Vickers indent. 527 HV10. Nital etch. 200X

4.4 Tensile Testing

The engineering stress-strain curves for different holding times at 260°C are presented in Figure 4-20. The result of changing the holding time from 0.5h to 2h, results in a drastic increase in elongation. A holding time of 10h result in a higher yield strength but a lower UTS, compared to 2 hours. The key data for all tensile tests are listed in Table 4-2.

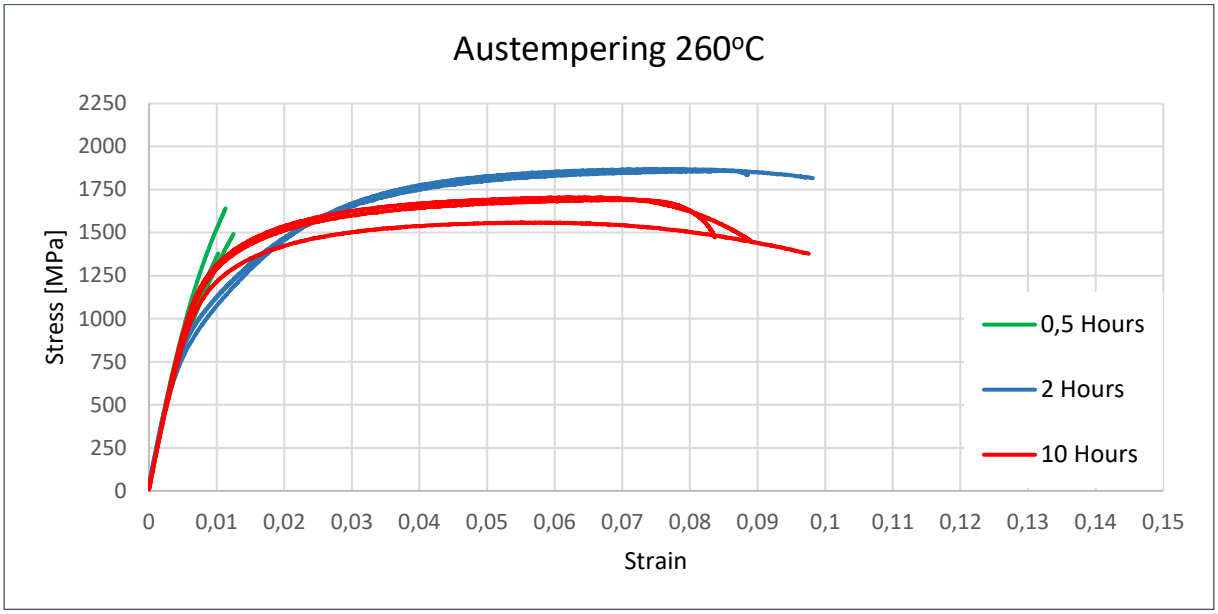

Figure 4-20 Engineering stress-strain curve for 9022 steel, austempered at 260°C.

The engineering stress-strain curves for different holding times at 280°C are presented in Figure 4-21. In this graph, the same change in elongation between 0.5 hours and 2 hours is observed. The trend of a holding time of 10 hours, resulting in higher yield strength, is also present and there does not seem to be a noticeable difference in UTS.

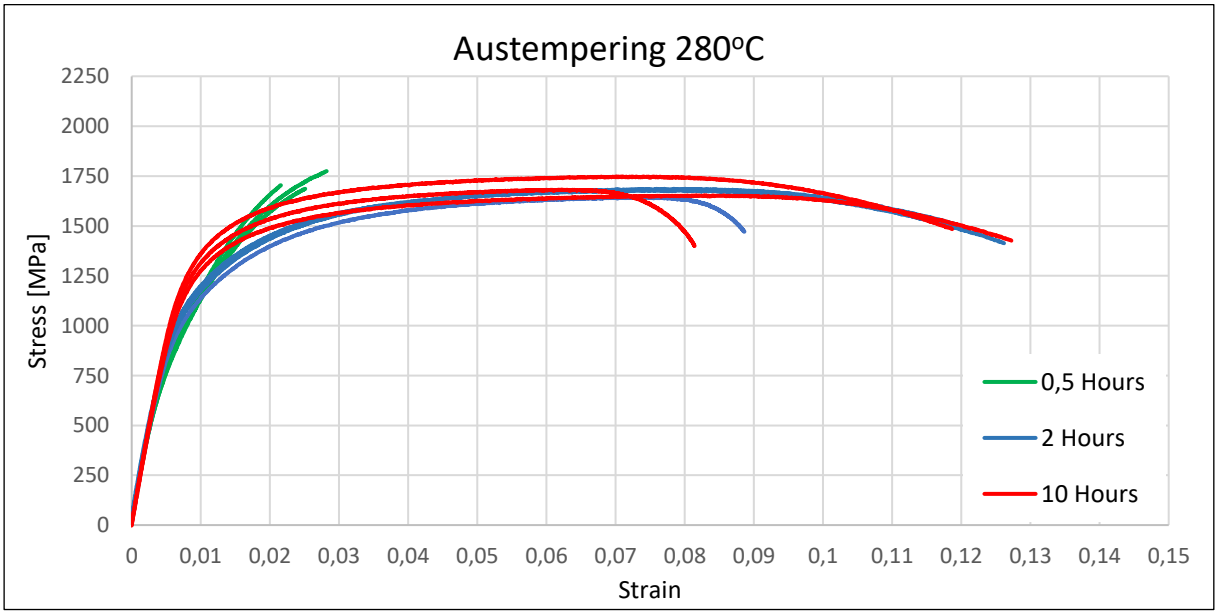

Figure 4-21 Engineering stress-strain curve for 9022 steel austempered at 280°C.

The engineering stress-strain curves for samples austempered at 300°C for 2 hours, are presented in Figure 4-22. The properties are similar to 2 hours at 280°C.

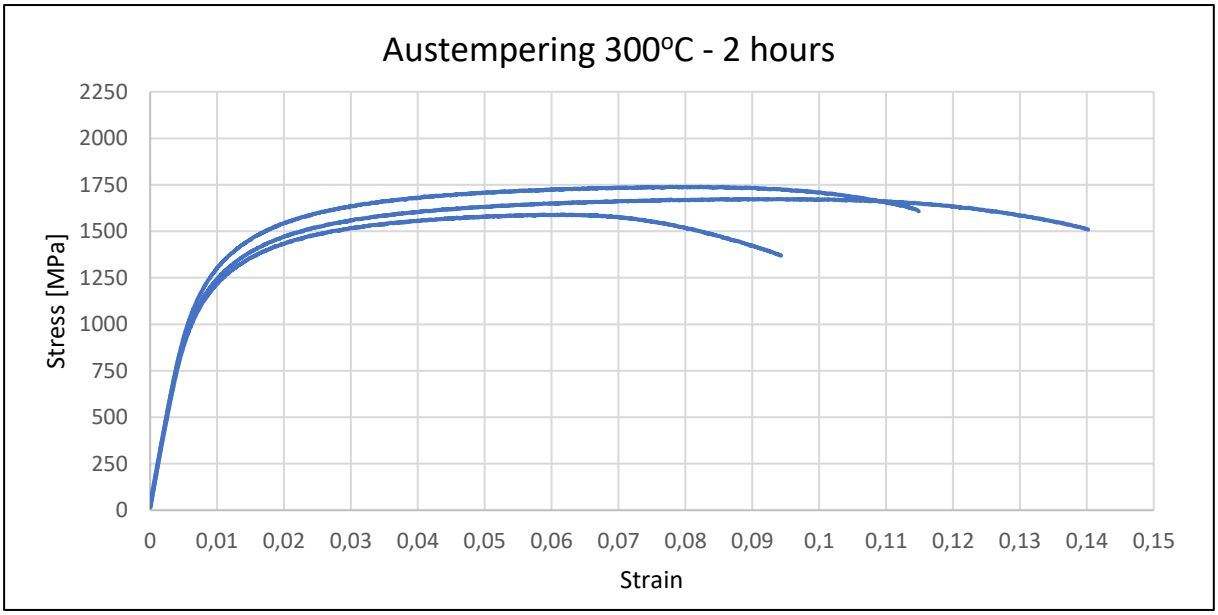

Figure 4-22 Engineering stress-strain curve for 9022 steel austempered at 300°C.

The engineering stress-strain curves for different holding times at 400°C are presented in Figure 4-23. The samples are very brittle, with no relevant difference in properties based on holding time.

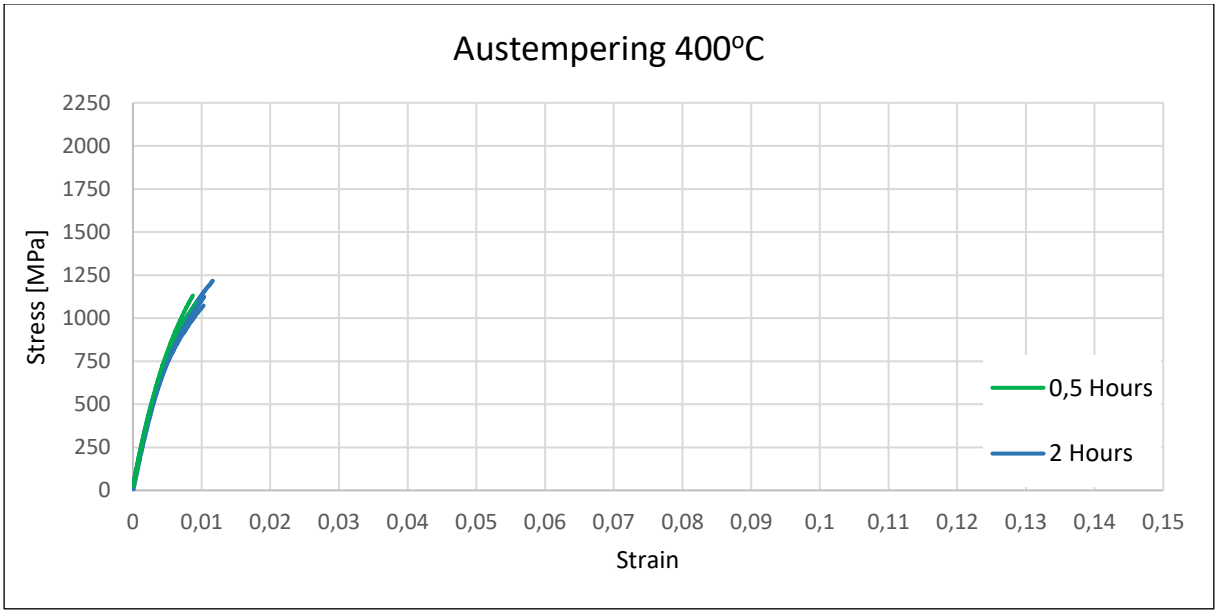

Figure 4-23 Engineering stress-strain curve for 9022 steel austempered at 400°C.

In Figure 4-24, the engineering stress-strain curves for martensitic samples, with different tempering, are presented. The tempered samples are all held for 1 hour at their respective temperatures. The ductility increases with tempering temperature up to 250°C. A tempering temperature of 450°C result in very low ductility that hardly exceeds the yield point.

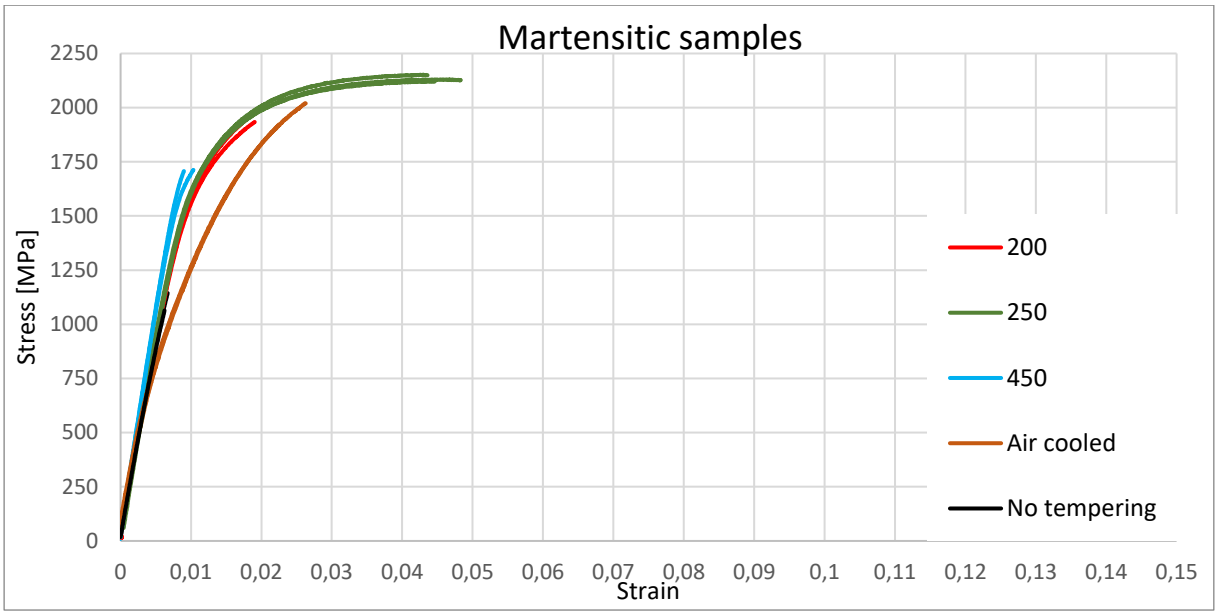

Figure 4-24 Stress-strain curve for different tempering temperatures [ºC].

The engineering stress-strain curve for the reference steel is presented in Figure 4-25 and shows a yield strength of 1240 MPa and UTS of about 1700 MPa. The elongation was considerably higher than the elongation of martensitic 9022, tempered at 200ºC.

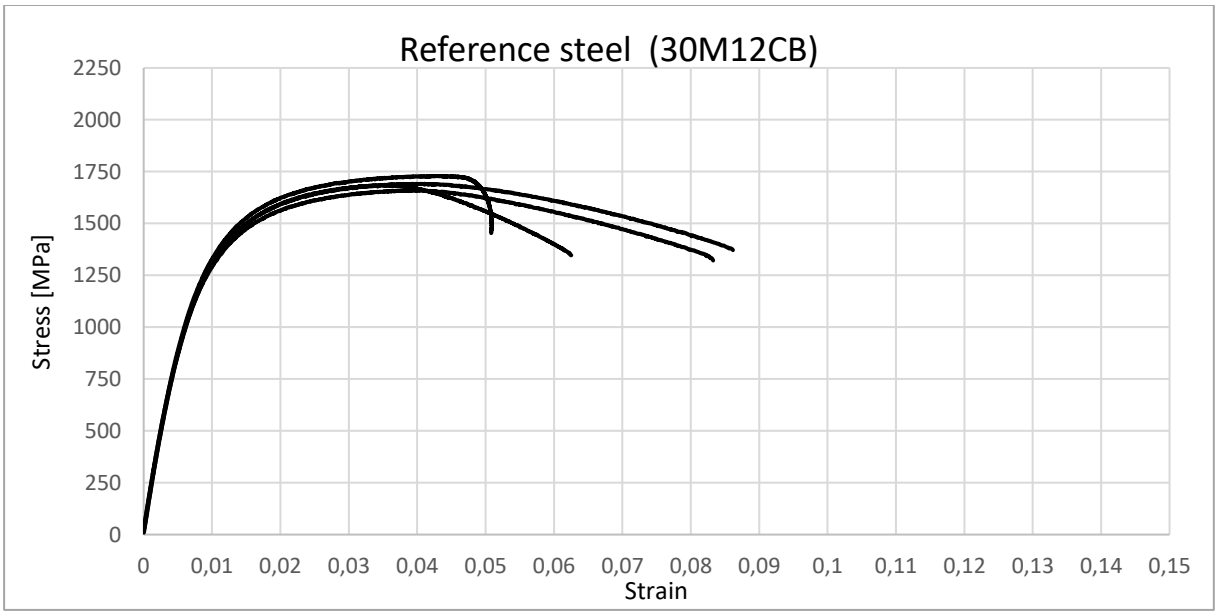

Figure 4-25 Stress-strain curve for 30M12CB.

The key data from the tensile tests are presented in Table 4-2. The values are given by the MTS-tensile test software "TestSuite", with exception of the results marked by "*", which are results from previous work [3].

Table 4-2 Key data from tensile testing. Values are given by MTS-tensile test software.

Austempering [°C]	**Holding time [hours]**	**Yield strength [MPa]**	**Ultimate tensile strength [MPa]**	**Strain at fracture [%]**
260	0.5	1352	1503	1.1
	2	1071	1863	9
	10	1206	1651	9
280	0.5	1123	1722	2.5
	2	1058	1644	11.2
	10	1249	1694	10.7
300	2	1162	1667	11.6
400	0.5	-	1019	0.8
	2	958	1138	1.1
Tempered martensite [°C]				
Quenched*	-	-	1100	0.6
200*	1	1700	1950	1.9
250*	1	1700	2120	4.5
450	1	1622	1703	0.9
Air-cooled	-	1339	1971	2.5
Reference (30M12CB - quenched)	-	1240	1692	7.1

4.5 Charpy Impact Testing

In Table 4-3, the results from Charpy impact testing are presented. The raw data can be found in Appendix C. The samples 280°C – 2h, 280°C – 10h, and 300°C – 2h, have the highest absorbed energy of 33 - 34 J, while the quenched sample without temper has the lowest absorbed energy of, 1.9 J.

Table 4-3 Results from Charpy impact testing.

Sample	**Average absorbed energy [J]**
260°C – 2h	25.4
280°C – 0.5h	16.6
280°C – 2h	34.2
280°C – 10h	34.4
300°C – 2h	32.8
Tempered martensite 200°C – 1h*	3.9
Tempered martensite 250°C – 1h*	6.3
Tempered martensite 450°C – 1h	4.9
Quenched, no temper*	1.9
Air-cooled	8.5
Reference	29.1

4.6 Retained Austenite

The first attempt at identifying retained austenite was done using EBSD on mechanically polished samples. As presented in Figure 4-26, at 500X the retained austenite (shown with red pixels) appears to be homogeneously distributed without any coalescence. Post processing with a confidence index of 0.08 was conducted, illustrated in Figure 4-27. At 2500X, there are some patterns in the distribution of retained austenite, but as seen in Figure 4-27 it does not appear as particles or defined areasFigure 4-28. As visible in Figure 4-29, applying a confidence index of 0.08, result in the same observations as Figure 4-27.

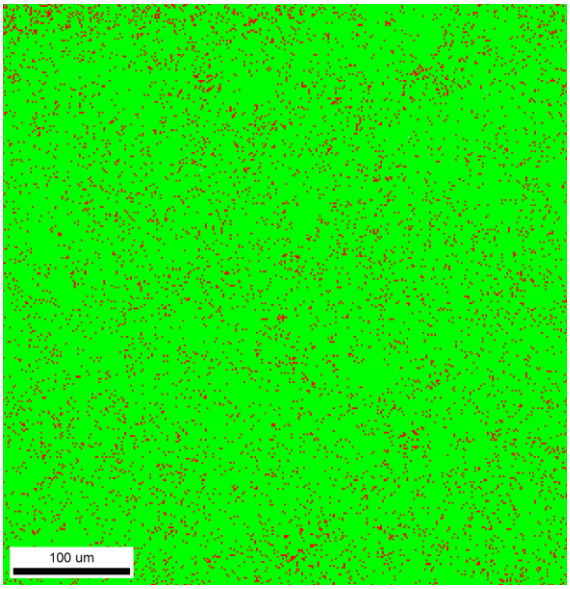

Figure 4-26 Sample 280 – 0,5h. EBSD-map of austenite (red) and ferrite (green). 6.6% austenite and 93.4% ferrite. Settings: 500 X, step size 1.5 µm,17 kV

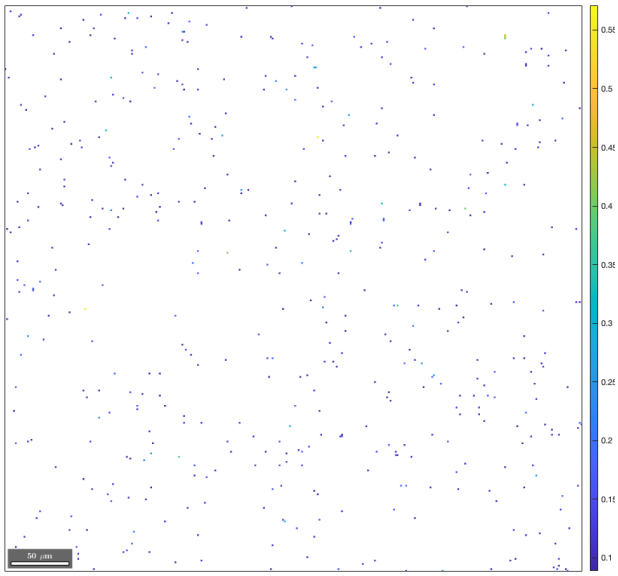

Figure 4-27 Figure 4-26 filtered with confidence index 0.08. Using MTEX toolbox. 500 X

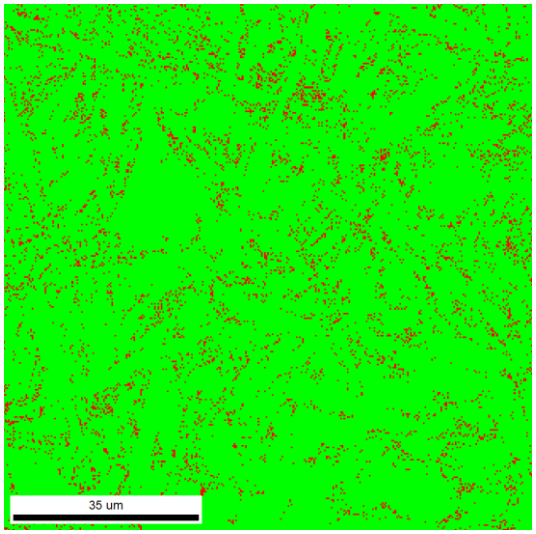

Figure 4-28 Sample 280 – 0,5h. EBSD-map of austenite (red) and ferrite (green). 6.3%

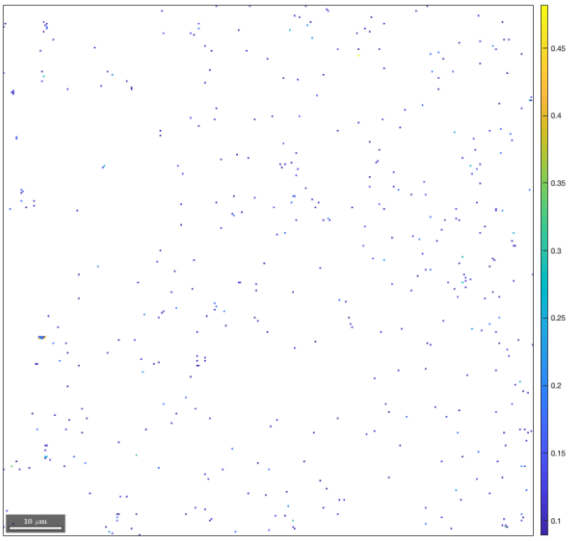

Figure 4-29 Figure 4-28filtered with confidence index 0.08. Using MTEX toolbox. 2500 X

austenite and 93.7% ferrite. Settings: 2500 X, step size 0.3 µm, 17 kV,

The amount of retained austenite was also examined using XRD, as presented in Table 4-4. Note that these samples were electropolished as their final step, as opposed to the samples in Figure 4-26 to Figure 4-29, which were polished mechanically with OP-S.

Table 4-4 The fraction of retained austenite for samples austempered at 280°C, for holding times 0.5, 2, and 10 hours obtained from XRD. The results show larger amounts of retained austenite as the holding time increases from 0.5 h to 2 h, with a reduction from 2 h to 10 h.

Holding time at 280°C	**Fraction of retained austenite [%]**
0.5	14
2	18
10	15

In Figure 4-30 and Figure 4-31, the retained austenite is visible as the light areas. The retained austenite is located in "blocks" and thin films between the bainite laths.

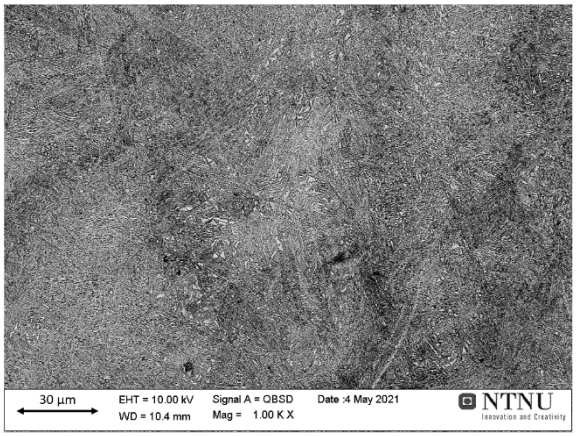

Figure 4-30 BSE image of 280°C – 2h. Electropolished. 1000X

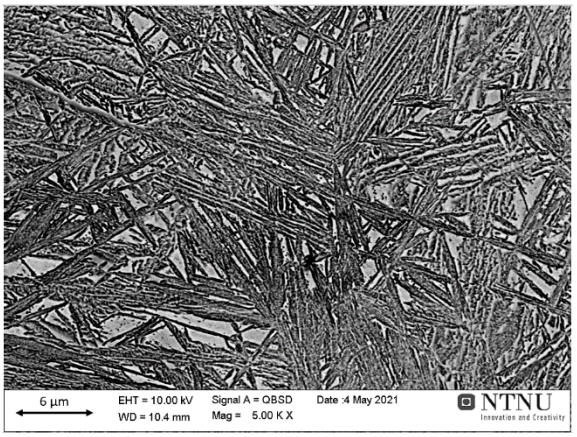

Figure 4-31 BSE image of 280°C – 2h. Electropolished. 5000X

4.7 Simulated Transformation Temperatures

The manufacturer of the examined steel provided a calculated TTT-diagram. The program that was used only allows for maximum 2.5 wt% Si.

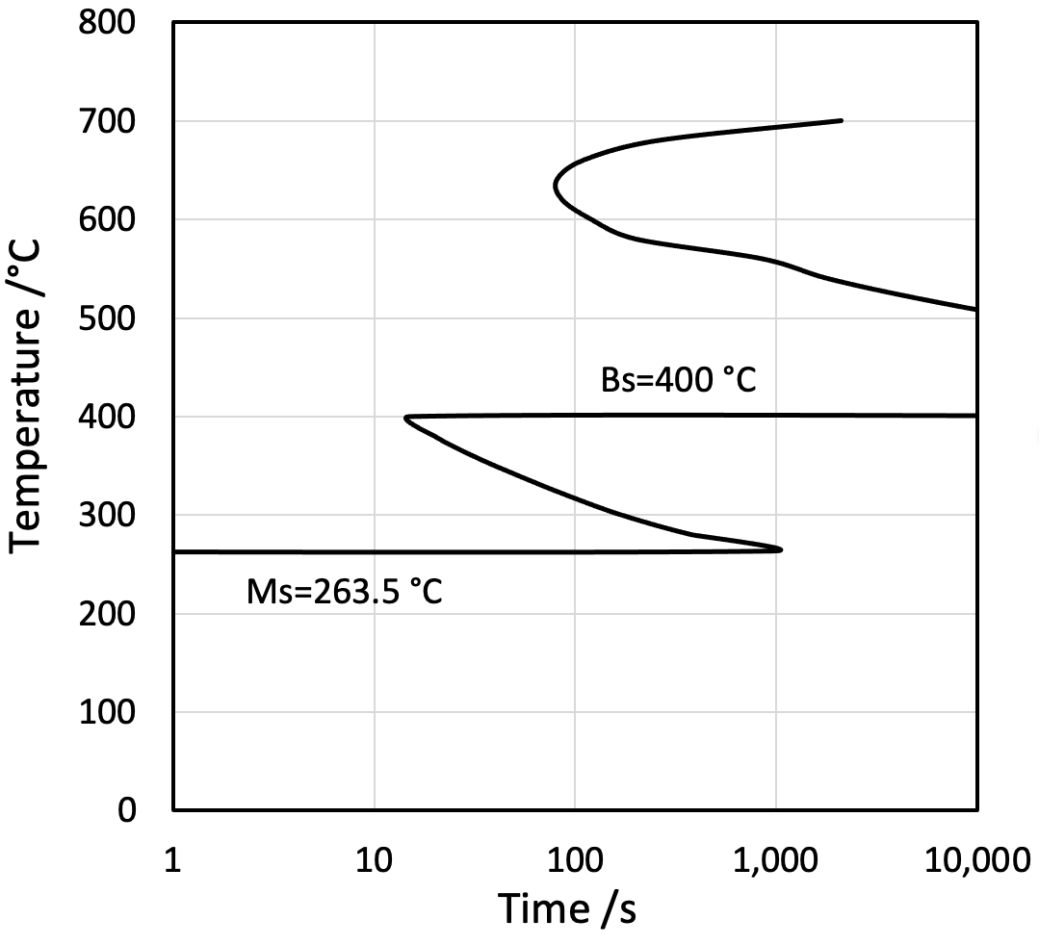

Figure 4-32 Calculated TTT-diagram, as provided by Ovako.

To get some insight on the importance of calculating the TT-diagram with lower Si-content, the author calculated the transformation temperatures using MAP_STEEL_MUCG83 [24] , created by H.K.D.H. Bhadeshia. The chemical composition was set to the values provided by Ovako, and the Si-content was varied.

Table 4-5 The calculated transformation temperatures of the 9022, with different Si-content.

	2.5% Si	**1% Si**	**0% Si**
M_s	263	263	263
Nucleation limited bainite start [°C]	370	370	370
Growth limited bainite start [°C]	435	433	431
Widmanstätten ferrite start [°C]	370	370	370

5 Discussion

In this work, the mechanical properties of the 9022-prototype steel for different heat treatments have been examined. Specifically, the difference between tempered martensite and bainite has been in focus. Austempering is a more complex and expensive heat treatment than a simple quench. However, depending on the requirements of the particular part, it can be a worthwhile investment. If the hardness between the martensitic and bainitic sample is the same, bainite can achieve higher fracture toughness and elongation [9].

Identifying the influence of austempering time and temperature on the final properties is a crucial part of designing a production process. The optimal production process does not necessarily result in the absolute best mechanical properties, but it balances the mechanical properties with other factors like complexity, cost, time, and robustness to deviations in time and temperature. Bhadesia [25], achieved a bainitic steel with excellent mechanical properties with isothermal holding at low temperatures for up to 60 days. This processing time cannot be justified in an industrial application. The holding times of 0.5 – 24 h were chosen to strike a balance with the scientific examination while remaining relevant for a potential production process.

5.1 Austempering

The initial part of this work was to measure Vickers hardness of samples held for 0.5, 2, 10, and 24 hours, at temperatures between 260 and 400°C, increasing in increments of 20°C. This experiment was done to get a broad overview of the influence of temperature and time. The results are presented in section 4.2. In the first experimental plan, 280°C was the lowest temperature because the martensitic start temperature was found to be 270°C experimentally and 263°C by calculation, see Figure 4-4 and Figure 4-32. Austempering at 260°C was done after it was revealed that 280°C might be the optimal heat treatment to get insight into the temperature dependence of the process.

The increase in Si-content in the segregation bands result in different transformation characteristics, requiring higher temperatures for austenitizing and slowing down phase transformations during cooling. As found in the previous work [3], the brighter areas contain more Si. In Figure 4-14, the light areas overlap with the martensitic microstructure. This is a source of uncertainty, both regarding imaging and hardness measurements. To mitigate the effect of the segregation bands, several hardness measurements were taken perpendicular to the bands. Despite the challenges mentioned, as the measurements are aggregated in Figure 4-5, clear trends appear. The hardness measurements show that austempering temperature has a pronounced influence on hardness.

Depending on the austempering temperature, there appear to be two different transformation characteristics. Samples that were austempered at 260 – 360°C follow the

same two trends: a drop in hardness between 0.5 and 2 h and lower hardness with higher austempering temperature. On the other hand, this trend inverses for the samples held at 380 and 400°C; holding for 2 hours results in higher hardness, and increasing austempering temperature leads to higher hardness.

The increase in hardness for austempering at 400°C was not expected, and further examination was conducted to get a better insight. Figure 4-14 to Figure 4-17, show that the microstructure consists of two phases: dark coarse needles and finer white/brown needles. The large difference in microhardness suggests that these phases are upper bainite and martensite. Considering that martensite is usually formed at high cooling rates, the fact that a higher austempering temperature leads to more martensite is perhaps counterintuitive. However, Figure 4-32 offers a possible explanation; at 400°C the temperature is in between the pearlite and the bainite nose in the TTT-diagram, resulting in a low driving force for the bainitic transformation, and the temperature is too low for the austenite to transform to ferrite/pearlite. The end result is upper bainite and a large amount of unstable retained austenite.

After the samples are removed from the salt bath, the retained austenite is transformed into martensite. The samples held at 24h, have a significant drop in hardness. Figure 4-18 and Figure 4-19, show the different size of the indentation, as well as the surrounding microstructure, for samples held at 400°C for 2 and 24 h, respectively. The sample that has been austempered for 24 hours has a higher concentration of the dark coarse needles and the other present phase does not have the same appearance as the martensite in Figure 4-18. The appearance and lower measured hardness indicate that the white phase is retained austenite. The long holding time has most likely compensated for the low driving force, producing upper bainite and a carbon enriched retained austenite. This would be in accordance with the incomplete reaction phenomena, discussed in chapter 2.4.1.

The hardness of the reference steel was measured and used as the minimum hardness requirement for the austempered samples. The samples that were austempered at 260 - 300 and 400°C, were the only samples with sufficient hardness.

5.2 Retained Austenite

The presence and morphology of retained austenite is a key influence of the properties of high Si carbide-free bainitic steels. The high silicon content hinders carbide precipitation between the bainite laths, and instead, a carbon enriched retained austenite film separates the bainite laths. The retained austenite film is highly advantageous to mechanical properties, improving both toughness and elongation. Retained austenite improves the mechanical properties by two different mechanisms; the high formability of austenite makes it capable of absorbing impact energy and mitigate crack propagation, and the different crystal structure between austenite and ferrite hinders dislocation movement [26].

The first attempt of characterizing retained austenite was made using EBSD, as seen in Figure 4-26 to Figure 4-29. The accuracy of these results is questionable; the retained austenite does not appear to have any structure but is dispersed as single pixels throughout the sample. In Figure 4-28 there appears to be some structure to the

dispersion of retained austenite, but there is no clearly visible structure. The reason for this might be that the step size, 0.3 µm, was too long to accurately identify the retained austenite film. According to Bhadeshia and Edmonds [10], the retained austenite films have a thickness of approximately 0.125 µm. Pashangeh, Zarchi [27] reported that EBSD is in many cases not capable of separating martensite and finely distributed retained austenite, especially in the blocky retained austenite/martensite islands.

Based on literature [7, 11, 26] and Figure 4-31, blocks of retained austenite would be expected. Note that these images have different holding times, EBSD is 0.5h, and BSE is 2h. The lack of blocky austenite in the EBSD-acquisition, might be caused by the retained austenite transforming to martensite during the mechanical polishing prior to analysis. In a three-body abrasion wear experiment of CFB, the retained austenite was measured before and after the experiment, where they found a reduction from 17% to <3% [28]. This would indicate that the retained austenite films also have transformed.

XRD is a common and accurate technique for identifying the amounts of retained austenite [29]. The XRD measurements were conducted on samples held at 280°C. From Table 4-4, the amount of retained austenite is shown to be higher for samples held for 2h compared to 0.5h. During austempering, carbon diffuse from the forming bainite to the surrounding austenite. The increased holding time allows more carbon to diffuse, further stabilizing the austenite. For the sample austempered for 0.5h, the austenite is not sufficiently stabilized, causing it to transform to martensite during cooling. This hypothesis is supported by Charpy impact testing, the 280°C – 0.5h had about half the absorbed energy of 280°C-2h. It is also reflected in hardness measurements, the samples held for 0.5h consistently exhibit higher hardness than 2 h.

In Figure 4-30 and Figure 4-31, BSE images of the same electropolished samples used for XRD are shown. The suspected retained austenite is visible as brighter blocks or needles between bainite. From these images it is hard to conclude what the fraction of martensite and austenite is in the blocks. It would be advantageous to explore this further, but this was severely restricted due to technical issues with the SEMs.

5.3 Mechanical Properties

Mechanical testing is the central part of this work. Hardness measurements, tensile-and Charpy impact tests have been used to get an overview of the impact of different heat treatments. These are the most common experiments used to characterize the mechanical properties of a steel. As mentioned above, the samples with austempering at 260 - 300 and 400°C, were the only ones with hardness higher than the quenched reference steel.

The 9022 steel is a high strength steel with high hardenability. As with all steels, the heat treatment is vital to achieving the desired properties. The aim is to be able to identify processes and correlation by comparing a range of different austempering treatments. The results will also be compared to the mechanical properties of 9022 with a martensitic microstructure and the reference steel, quenched 30M12CB, that is used in production at this time.

The results from the mechanical testing are in line with the expected results, and there does not appear to be any major sources of error. There are of course always improvements that can be made. Due to time and cost, the samples were machined prior to heat treatment. Ideally, the samples would be fine machined after heat treatment, to reduce decarburization of the surface, potential deviations in geometry, and ensure a good surface finish.

5.3.1 Tensile Testing

The hardness measurements in Table 4-1 indicated that austempering for 2 hours at 280°C could be the optimal heat treatment. With this assumption in mind, the further experimentation was planned. Due to cost and time constraints, there were limitations to the number of samples that could be tested. For tensile testing, 9 different austempering procedures were tested, one with air-cooling, and one martensitic, tempered at 450°C, were tested. Each heat treatment had 3 parallels. The rest of the results were obtained from previous work [3]. Tensile testing of the bainitic samples had two goals. The first, and most important, was to examine the tensile properties of bainite, and the second was to identify the impact of changes in time and temperature.

The results of tensile testing in the temperature range of 260 to 300°C, shows that the samples with the same holding time are more similar than the samples with the same temperature. For this reason, the comparison is structured to compare the impact of temperature for a given holding time, as opposed to comparing the difference in holding time at a given temperature.

Austempering for 0.5 hours results in a sample with high hardness and yield strength. However, the steel is brittle, exhibiting strain at fracture of 1.1% for 260°C and 2.5% for 280°C. The absorbed energy in Charpy impact testing for 280°C – 0.5h, 16.6 J, was about half compared to 2h, 34.4 J. Considering these results, in addition to XRD showing higher concentrations of retained austenite for samples held for 2h compared to 0.5h, it is likely that the holding time was too short to stabilize the retained austenite, resulting in a large amount of martensite.

The samples held for 2 hours have a remarkable improvement in elongation before fracture. The result of increasing holding temperature was a reduction of UTS from 1860 MPa (260°C) to 1650 MPa (280 and 300°C), and there are also changes in the shape of the curves. The yield point of the samples held at 260°C is lower and less defined, with a much higher strain hardening rate, compared to 280°C. One possible explanation for this is a more pronounced TRIP-effect, caused by larger amount of retained austenite [15, 25]. The retained austenite has lower tensile strength and high ductility, causing the observed effect [11, 26]. As the sample is deformed, the retained austenite transforms into martensite, further increasing the strength. For this reason, the difference in yield strength is much greater than the difference in UTS. In the case of 260°C – 2h and 260°C – 10h, the yield strength of 2h was 130MPa lower than 10h and the UTS was 200MPA higher.

In terms of UTS and total elongation, the samples that were held for 10 hours have similar properties compared to 2h. The samples have a higher yield strength and lower rates of strain hardening.

The samples held at 400°C have properties that are similar to quenched and untempered martensite. The sample held for 2 hours has some plastic deformation prior to fracture, while 0.5h goes directly from elastic deformation to fracture. This supports the hypothesis that the microstructure contains upper bainite and martensite. A microstructure with these properties would be useless for the relevant applications, and therefore no further testing was conducted.

The martensitic samples of 9022 had significantly lower elongation at fracture, but higher yield strength and UTS. Among the martensitic samples there were two that stood out, quenched in water then tempered at 250°C and air-cooled. They had better elongation and UTS. The relevance of the mechanical properties of the air-cooled sample is restricted, because the dimensions of a sample are essential to the cooling rate.

In order to find a tempering that resulted in similar hardness to 280°C – 2 h, tempering at different temperatures of 350 – 500°C was conducted. A tempering temperature of 450°C resulted in a hardness of 572 HV10, compared to 573 HV10 for 280°C – 2h. The tempering at 450°C, resulted in a substantial reduction in elongation during tensile testing compared to 250°C. This might be caused by tempered martensite embrittlement (TME), which is a phenomenon where the tempering of martensite at higher temperatures causes it to become more brittle. There are two possible explanations for the mechanisms behind it. One explanation could be that tempering causes the high carbon retained austenite to decompose into cementite and a brittle martensite [25]. This could be studied by performing another temper. The other explanation is that the high temperature causes impurities like P, S, Sb, Sn, and N to segregate to the prior austenite grain boundaries [30].

This sample was originally included to compare the difference in mechanical properties between a martensitic and bainitic microstructure with the same hardness. The significant embrittlement of these samples reduces the value of the comparison. The bainitic samples were far superior in all aspects, except yield strength. The tempered martensite had a significantly higher yield strength of 1622 MPa, compared to 1058 MPa for 280°C-2h.

5.3.2 Charpy Impact Testing

Charpy impact testing revealed similar properties for the samples 2 h and 10h at 280°C, and 2 h at 300°C, with absorbed energy around 33 J. Considering that the Charpy samples were machined prior to heat treatment, and that only 3 samples were tested in each heat treatment, it is not possible to differentiate them further. The samples held for 2h at 260°C and 0.5h at 280°C, exhibited considerably lower absorbed energy, 25 J and 17 J, respectively.

Compared to the samples with martensitic microstructure, bainite had far superior properties. Among the samples that were not austempered, air-cooling had the highest absorbed energy of 8.5 J. Based on the CCT-diagram, tensile test, and absorbed energy; it is most likely that air-cooling results in a martensitic microstructure. The quenched and tempered sample with the highest absorbed energy, was tempered at 200°C and had an impact absorption of 6.3 J. The poor absorbed energy of the samples tempered at 450°C supports the hypothesis about TME discussed in 5.3.1.

5.4 Comparison with Reference Steel

The hardness of the quenched 30M12CB, was 540 HV10, and was set as a minimum hardness requirement for the part. The mechanical testing supports choosing austempering for 2 hours at 280°C as the optimal heat treatment. There were other samples that had higher or similar properties in specific tests. Both 10h at 280°C and 2h at 300°C, had higher yield strength. The hardness of 280°C – 10h fulfill the requirement, however, the increased austempering would make it less practical for industrial purpose. Austempering at 300°C for 2 hours, results in a hardness of 551 HV10, which also is within the requirement. The main reason 300°C – 2h was disqualified, was due to the robustness regarding deviations in temperature. During production, it is important to have a margin for error, and if 300°C – 2h was chosen, an increase in temperature of 20°C would result in a part below the threshold. Finally, 280°C for 2 hours is one of the samples with the highest hardness, which has shown to be strongly related to wear resistance [19].

The measured properties of 9022 (280°C – 2h) and 30M12CB (quenched), is presented in Table 5-1. The steels have similar UTS, while 30M12CB has higher yield strength and 9022 has higher hardness, better strain at fracture, and absorbed energy in the Charpy impact test. The retained austenite in 9022 (280°C – 2h) was measured with XRD to be 18%. 30M12CB (quenched) has not been measured but is assumed to be low.

Table 5-1 Table of the mechanical properties of 9022 (280°C – 2h) and 30M12CB (quenched).

Steel	**Yield strength [MPa]**	**UTS [MPa]**	**Strain at fracture [%]**	**HV10**	**Charpy impact [J]**
9022 (280°C-2h)	1058	1644	11.2	573	34.2
30M12CB (quenched)	1240	1692	7.1	540	29.1

Shah and Das Bakshi [28], compared the specific wear rates in three-body abrasive wear for CFB, martensite, and bainite-martensite structures of similar hardness. They found that the specific wear rate of CFB was about half that of martensite. They also found that the mechanisms of wear were different for martensite and CFB. In the case of martensite, fragmentation and chipping was the prominent wear mechanism. CFB was worn by a combination of grooving and minor pitting; it also showed significant plastic deformation. The retained austenite also had the TRIP effect discussed in section 2.4.1. with a reduction in retained austenite from 17% to <3%. The retained austenite transforms into a hard martensite during deformation. The martensite transformation can have two effects: improving wear resistance by achieving higher hardness on the active surface layer while retaining the ductile properties underneath, and the volume increase associated with the martensite transformation. The volume increase causes local compressive stress on the surface, hindering the creation and propagation of cracks, further improving wear resistance [21]. Leiro, Vuorinen [31] also found similar reductions in wear rate for sliding wear between CFB and a reference steel with a lower bainite

microstructure. They concluded that the TRIP-effect in the CFB was the reason for this increase.

The prospect of a two-fold increase in wear resistance would be promising and worth exploring further. However, there are other considerations that must be made before the steel can be implemented for mass production. Martensitic parts can be produced by one-piece flow, where parts can be continuously forged and quenched. Switching to an austempering process would require a more batch-like process, austempering the parts in salt baths for 2 hours. The austempering in salt baths is most relevant for small parts, as it is easier to control cooling rates throughout the part. The impact of such factors will vary widely for different production lines and must be made according to the specific conditions of the situation. In some cases, it can be a bottleneck detrimental to the whole production line. In other cases, the cost increase could be negligible.

6 Conclusion

In this work, the prototype steel 9022 was examined. The impact of different austempering temperatures and times, on microstructure and mechanical properties, of different austempering temperatures and times, was studied. The same mechanical testing was conducted on air-cooled samples, tempered- and untempered- martensite.

- There appear to be two different transformation characteristics based on the austempering temperature:
    - Samples austempered at 260 to 360°C, show a reduction in hardness with increasing austempering temperature and increasing holding time from 0.5 h to 2 h. Further prolonging the holding time has a negligible impact.
    - For samples austempered at 380 and 400°C, these trends are inversed. 400°C was the highest austempering temperature, and it also exhibited the highest hardness. Further, increasing the holding time from 0.5 to 2 h caused a significant increase in hardness. The reason for the increased hardness for 400°C could be that the driving force for the bainitic reaction is too low, resulting in a large amount of unstable retained austenite, that transforms into martensite during cooling. This is supported by LOM, SEM, and microhardness.
- Mechanical testing of the austempered samples revealed a significant improvement in energy absorption for Charpy impact tests and strain at fracture, compared to tempered martensite. However, the martensitic samples had higher hardness, yield strength, and UTS.
- By aggregating these results and considering the practical aspects, it was found that austempering at 280°C for 2 h would achieve a good combination of mechanical properties, reasonable processing time, and robustness to deviations in temperature and time. The strain at fracture was more than twice that of martensite tempered at 250°C. This austempering also result in the highest amount of retained austenite and shows a strong indication of the TRIP-effect during tensile testing, which has been shown to increase abrasive wear resistance.
- XRD revealed higher amounts of retained austenite for the 280°C – 2 h sample, compared to 280°C. Prolonging the austempering from 0.5 to 2 h, increased the retained austenite from 14 to 18 %.
- The mechanical properties of the austempered 9022 steel are promising and worth exploring further. If the 9022 steel exhibit good abrasive resistance in the conditions that the knock-on holder is subjected to, it would be highly relevant for production. However, before a final decision can be made on the implementation of austempered 9022, more research and optimization must be conducted.

7 Further Work

In order to implement the austempered 9022 steel for industrial applications, there are some areas that would benefit from further exploration:

- Further examination of the development and transformation of the retained austenite.
- Optimizing the heat treatment to reduce the blocky retained austenite. This would probably improve wear resistance.
- Conducting abrasive wear experiments that mimic the real-world conditions.

References

1. Nolte, D. *TailorPro - Skreddersydde materialegenskaper gjennom nye prosesseringsrutiner for høykvalitets stålprodukter*. 2020 14.12.20]; Available from: https://www.sintef.no/prosjekter/tailorpro-skreddersy-materialegenskaper-gjennom-nye-prosesseringsrutiner-for-hoykvalitets-stalprodukter2/.
2. Worup, C. *Kverneland sætter sagen på spidsen*. 2013 [cited 2020 07.12]; Available from: https://www.maskinbladet.dk/artikel/43694-kverneland-saetter-sagen-pa-spidsen.
3. Schawlann, S., *Characterization of a Prototype High Performance Steel*. 2020, NTNU.
4. Callister, W.D. and D.G. Rethwisch, *Materials science and engineering : an introduction*. 8th ed. 2010, Hoboken, NJ: John Wiley & Sons. xxiii, 885, 82 p.
5. Bhadeshia, H. and R. Honeycombe, *Steels : Microstructure and Properties, Fourth Edition*. 2017, Elsevier Science and Technology Books, Inc.,: Place of publication not identified. p. 1 online resource (490 pages).
6. Bleck, W., *Material science of steel, Textbook for Students at RWTH Aachen*. 2016, RWTH Aachen. 379.
7. Bhadeshia, H.K.D.H., *Nanostructured bainite.* Proceedings of the Royal Society A: Mathematical, Physical and Engineering Sciences, 2010. **466**(2113): p. 3-18.
8. Tian, J., et al., *Transformation Behavior and Properties of Carbide-Free Bainite Steels with Different Si Contents.* steel research international, 2019. **90**(3): p. 1800474.
9. Bhadeshia, H.K.D.H., *Bainite in Steels: Theory and Practice, Third Edition (3rd ed.)*. 2015: CRC Press.
10. Bhadeshia, H.K.D.H. and D.V. Edmonds, *Bainite in silicon steels: new composition–property approach Part 2.* Metal Science, 1983. **17**(9): p. 420-425.
11. Zhou, M., et al., *Effects of Austenitization Temperature and Compressive Stress During Bainitic Transformation on the Stability of Retained Austenite.* Transactions of the Indian Institute of Metals, 2017. **70**(6): p. 1447-1453.
12. Tan, Z.L., et al., *The Effect of Si on the Toughness of High Strength Mn-Si-Cr Series Bainitic Steels.* Materials Science Forum, 2005. **475-479**: p. 213-216.
13. Liu, B., et al., *The effect of retained austenite stability on impact-abrasion wear resistance in carbide-free bainitic steels.* Wear, 2019. **428-429**: p. 127-136.
14. Bhadeshia, H.K.D.H., *Some phase transformations in steels.* Materials Science and Technology, 1999. **15**(1): p. 22-29.
15. Solberg, J.K., *Teknologiske metaller og legeringer*. 2017, Trondheim.
16. Long, X.Y., et al., *Carbide-free bainite in medium carbon steel.* Materials & Design, 2014. **64**: p. 237-245.
17. Huang, H., M.Y. Sherif, and P.E.J. Rivera-Díaz-del-Castillo, *Combinatorial optimization of carbide-free bainitic nanostructures.* Acta Materialia, 2013. **61**(5): p. 1639-1647.
18. De Cooman, B.C., *11 - High Mn TWIP steel and medium Mn steel*, in *Automotive Steels*, R. Rana and S.B. Singh, Editors. 2017, Woodhead Publishing. p. 317-385.
19. Adam Hylén, S.L. and E.S. Patrik Ölund, *Understanding wear mechanisms – the application technology behind WR-Steel.*
20. Natsis, A., G. Petropoulos, and C. Pandazaras, *Influence of local soil conditions on mouldboard ploughshare abrasive wear.* Tribology International, 2008. **41**(3): p. 151-157.

21. Kumar, R., R.K. Dwivedi, and S. Ahmed, *Stability of Retained Austenite in Carbide Free Bainite during the Austempering Temperature and its Influence on Sliding Wear of High Silicon Steel.* Silicon, 2021. **13**(4): p. 1249-1259.
22. Pickering, E.J. and H.K.D.H. Bhadeshia, *Macrosegregation and Microstructural Evolution in a Pressure-Vessel Steel.* Metallurgical and Materials Transactions A, 2014. **45**(7): p. 2983-2997.
23. ISO, *Metallic materials — Charpy*

pendulum impact test 2016: Switzerland.
24. Mathew Peet , H.K.D.H.B., *MAP_STEEL_MUCG83*.
25. Hu, G.L., et al., *Mechanism of tempered bainite embrittlement in some structural steels.* Materials Science and Engineering: A, 1991. **141**(2): p. 221-227.
26. Bhadeshia, H.K.D.H. and D.V. Edmonds, *Bainite in silicon steels: new composition–property approach Part 1.* Metal Science, 1983. **17**(9): p. 411-419.
27. Pashangeh, S., et al., *Detection and Estimation of Retained Austenite in a High Strength Si-Bearing Bainite-Martensite-Retained Austenite Micro-Composite Steel after Quenching and Bainitic Holding (Q&B).* Metals, 2019. **9**: p. 492.
28. Shah, M. and S. Das Bakshi, *Three-body abrasive wear of carbide-free bainite, martensite and bainite-martensite structure of similar hardness.* Wear, 2018. **402-403**: p. 207-215.
29. Su, Y.Y., et al., *Retained Austenite Amount Determination Comparison in JIS SKD11 Steel Using Quantitative Metallography and X-Ray Diffraction Methods.* Advanced Materials Research, 2012. **482-484**: p. 1165-1168.
30. Minicucci, D., et al., *Tempered Bainite and Martensite Embrittlement in Microalloyed Steel for Forged Railroad Wheel to Heavy Haul Application.* Materials Research, 2021. **24**.
31. Leiro, A., et al., *Wear of nano-structured carbide-free bainitic steels under dry rolling–sliding conditions.* Wear, 2013. **298-299**: p. 42-47.

Appendices

7.1 A

Raw data from Charpy impact testing.

260 - 2h	280 - 0,5h	280 - 2h	280-10h	300 - 2h	Tempered 450	Air-cooled	Ref quenched 30M12CB
28,63	16,24	33,89	28,56	37,29	5,72	8,22	30,01
24,01	19,11	39,73	33,83	29,32	3,18	8,8	33,18
23,44	14,34	28,89	40,85	31,8	5,78	-	29,55
-	-	-	-	-	-	-	31,64
-	-	-	-	-	-	-	21,33
25,36	**16,56**	**34,17**	**34,41**	**32,80**	**4,89**	**8,51**	**29,14**

7.2 B

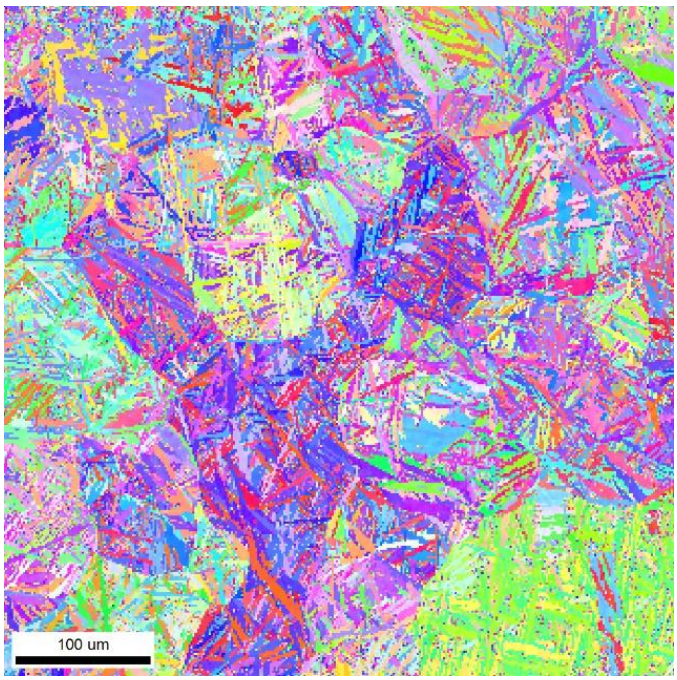

Inverse pole figure 280°C – 2 h. 500X Settings in 3.3.

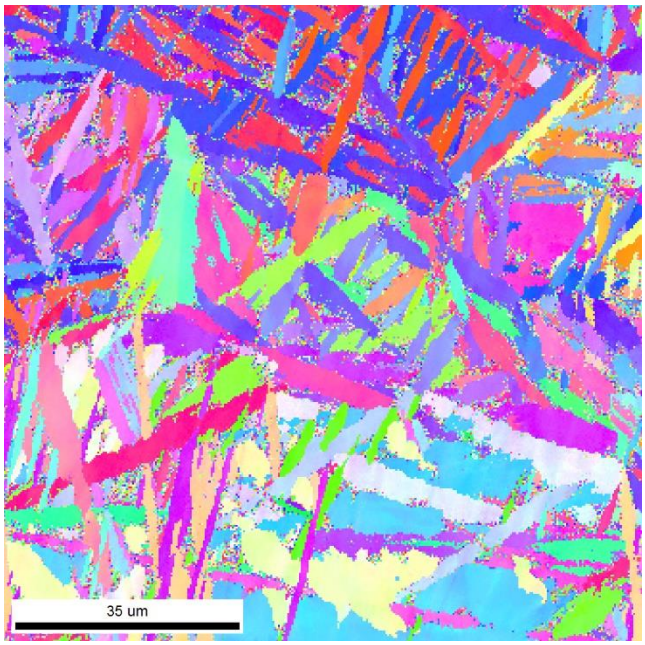

Inverse pole figure 280°C – 2 h. 500X Settings in 3.3

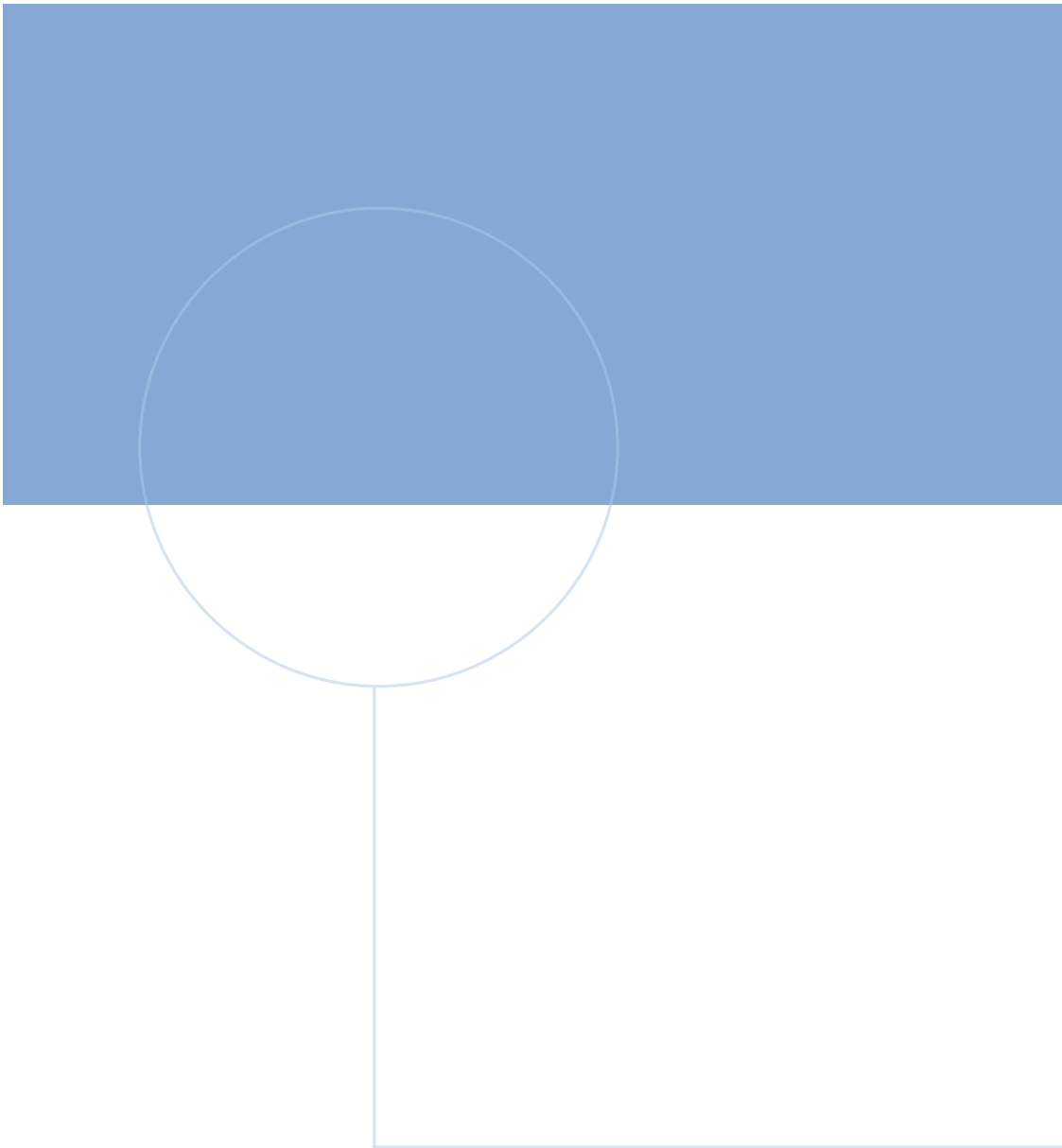

NTNU

Norwegian University of
Science and Technology